rijksuniversiteit groningen

SRON

Internship SRON

Analysing temperature behaviour & control of the LC-cooler

Intern: J.W. Zijlstra

Period: Jan-Apr 2018

Supervisor SRON: dr. ir. Gert de Lange & dr. Damian Audley

Supervisor RuG: prof. dr. Arjan van der Schaft

Contents

1. Introduction

On the 22nd of January I started my internship at SRON for the duration of 3 months. I was assigned the task to examine the temperature behaviour of the LC-cooler and implement a PID control system to control temperature fluctuations within set limits inside the LC-cooler.

1.1. SRON

SRON is a part of the Netherlands Organisation for Scientific Research (NWO). The Dutch institute is the national expertise institute for scientific space research. SRON has two locations, at the university complexes of Utrecht and Groningen with most of their employees situated in Utrecht.

They have often provided key contributions to instruments of missions of the major space agencies, ESA, NASA, and JAXA. These contributions have enabled the national and international space-research communities to explore the universe and to investigate the Earth's atmosphere and climate. As a national expertise institute, they stimulate collaboration between the science community, technological institutes, and industry.

1.2. LC-cooler

The TES-detectors (transition-edge sensor) currently being examined and tested at SRON operate at very low temperatures, i.e. in the order of a few kelvins. In order to reach these low temperatures a cryostat from Leiden Cryogenics, i.e. the LC-cooler, is operative at SRON's Groningen location. By means of a helium dilution of ^{3}He and ^{4}He, temperatures as low as 20 mK can be obtained. Inside the cooler multiple 'fixed' temperature levels are present, e.g. 20 mK, 120/150 mK and 700 mK as a part of the cooler operation process. A picture of the LC-cooler is displayed in Figure 2. The DM X-IFU device at the bottom of the LC-cooler is the test subject which has to be supplied with 3 temperature inputs, i.e. 50 mK, 300 mK and 2 K. As the 'fixed' temperature levels of the LC-cooler are not at the desired values low thermal conduction straps and heaters are being used between the levels to allow for temperature gradients. It is important that the supplied 50 mK temperature input does not fluctuate much as the TES-detector is highly sensitive to temperature changes. It is at the so-called critical temperature (Tc) where materials transition from the normal state to a superconducting state. The bandwidth at this critical temperature is very small, which emphasizes the importance to have a steady temperature input. As the LC-cooler is a coupled system, fluctuations in the 300 mK and 2 K stage could influence the 50 mK stage as well. Hence, it is important that all supplied values to the DM X-IFU device are steady temperature levels.

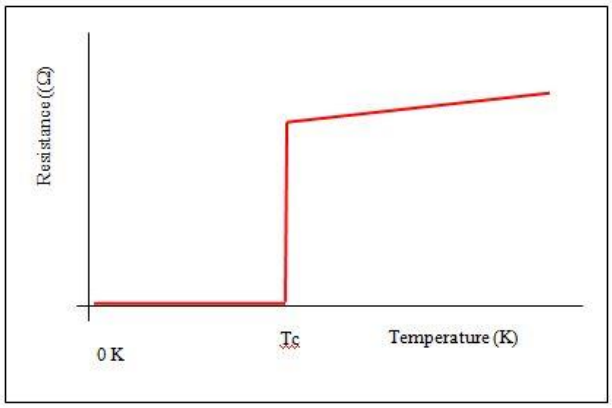

Fig. 1: At low temperatures (Tc) materials can obtain a superconducting state at which point the electrical resistance vanishes.

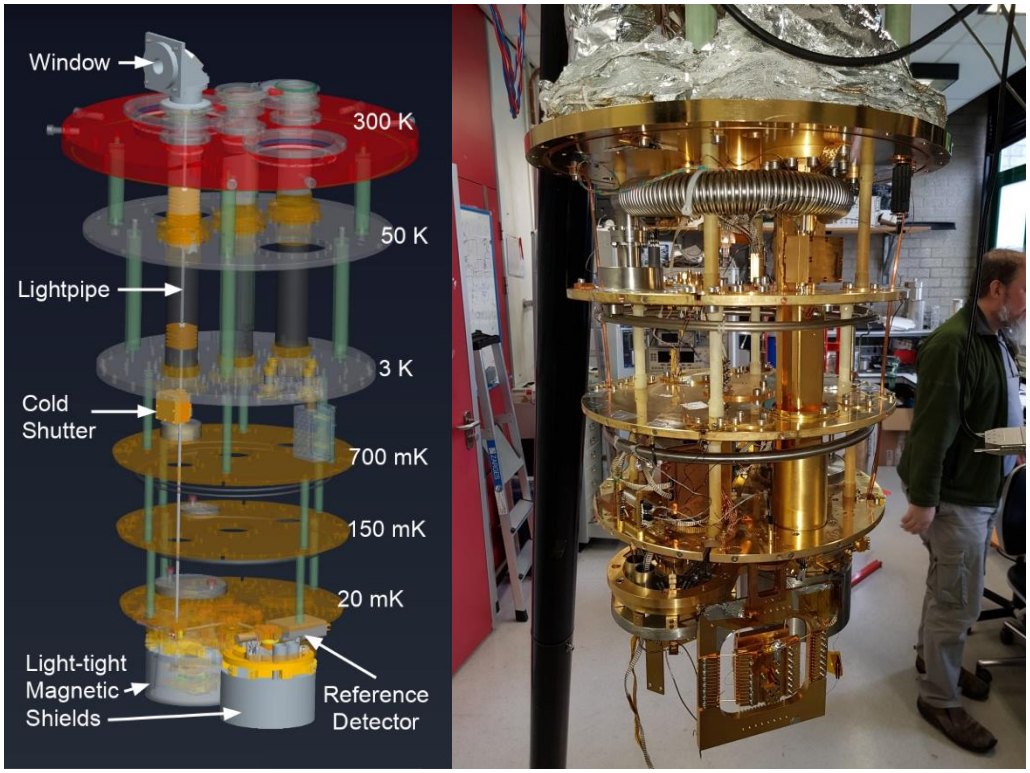

Fig. 2: Schematic (left side) and opened LC-cooler (right side).

On the right side in Figure 2 the LC-cooler is in the non-operating state which is also termed as being "warm". Only in this state can changes to the existing setup be made, e.g. placing new thermometers or replacing electrical components. Upon having done all necessary changes to the setup, the cooler is closed off again and it can take up to a few days before being "cold" again, i.e. the temperature ranges from 20 mK -3 K inside the inner vacuum chamber. For warming up the cooler it takes about the same time, 2-3 days, before being warm again.

It is important to note that not only Groningen is running experiments on the cooler, but also SRON's Utrecht location. As multiple groups are running simultaneous tests on the LC-cooler, SRON's desire is to have the cooler be operational as long as possible until multiple people indicate that changes have to be made. This makes it challenging for me as I am limited and/or dependent on others in getting measurements and changes done.

1.3. Problem description

As mentioned in section 1.2, where we described the operation process of the LC-cooler, 3 fixed temperature levels are obtained, i.e. 20 mK, 150 mK and 700 mK [see Figure 3]. Between these levels straps are placed to allow for temperature gradients as the X-IFU satellite operates at different temperature inputs, namely 50 mK, 300 mK and 2K for the reasons mentioned in 1.2. The assignment of this internship is to investigate the (temperature) behaviour of the straps (in particular the 700 mK strap) and to design a temperature control model to prevent temperature deviations in the X-IFU temperatures.

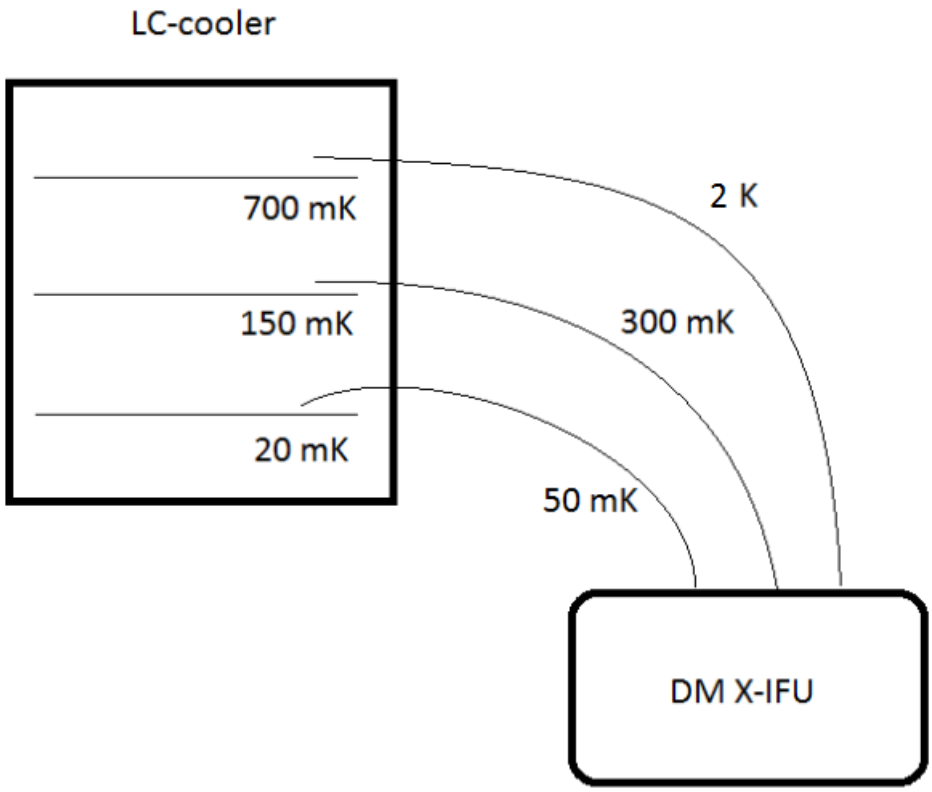

Fig. 3: Schematic overview of problem description.

2. Preliminaries: cryogenic behaviour

At room temperature material characteristics like thermal conductivity and specific heat can be considered constants, whereas at low temperatures (<50K) these properties become dependent of temperature. This complicates heat transfer modelling in materials as the equations describing the heat flow become non-linear. Hereto, it is important to fully understand what is happening with certain components in the LC-cooler, e.g. the 700 mK copper strap.

2.1. Heat transfer

Heat transfer (or heat) is thermal energy in transit due to a spatial temperature difference. Generally speaking, heat transfer takes place by any of the following processes: conduction, convection and/or thermal radiation. Convection occurs whenever a moving fluid and the underlying surface are at different temperatures from each other. Inside the LC-cooler it is a near-vacuum. As such, moving fluids are absent and heat cannot transfer by means of convection. The second option for heat transfer is through thermal radiation. All surfaces of finite temperature emit energy in the form of electromagnetic waves. There is however an upper limit to the emissive power, which is prescribed by the *Stefan-Boltzmann law*:

$$E_b = \sigma T_s^4$$

where T_s is the *absolute temperature* (K) of the surface and σ is the *Stefan-Boltzmann* constant ($\sigma = 5.67 \cdot 10^{-8}\ \frac{\mathrm{W}}{\mathrm{m^2K^4}}$). The surface of this upper limit is known as an ideal radiator or blackbody. As the emissive power depends on a fourth power of the absolute temperature, the thermal radiation becomes negligible at very low temperatures which are present in the LC-cooler. Hereto, the dominant process for heat transfer is conduction which will be discussed in the next section.

2.1.1. Thermal conductivity

Transfer of heat can also take place by means of conduction. In this case, heat transfers from the more energetic to the less energetic particles of a substance due to interactions between the particles. Plentiful examples exist where this phenomenon takes place, e.g. placing a pan on a lit stove or putting a spoon inside a cup of hot tea. This phenomenon can be described by the following formula for one-dimensional heat flow, which is also known as **Fourier's Law**:

$$q_x'' = -k\frac{dT}{dx}$$

where q_x'' (W/m^2) denotes the heat flux which describes the heat transfer rate in the *x* direction per unit area perpendicular to the direction of transfer. The heat rate by conduction, q_x , follows from taking the product of the flux and the area, $q_x = q_x'' \cdot A$. The parameter k is a transport property known as the **thermal conductivity** and is a characteristic of the material. For day-to-day life this parameter is a constant, however at low temperatures k becomes temperature dependent.

Closely related to thermal conductivity is **thermal resistance**. It is defined as the ratio of driving potential to the corresponding transfer rate:

$$R_{t,cond} \equiv \frac{T_1 - T_2}{q} = \frac{L}{kA},$$

with T_1, T_2 respectively the hot and cold end of the material and *L* the length of the material.

Heat can be carried by conduction *electrons* or by *lattice vibrations*, i.e. *phonons*. They are scattered by other electrons or phonons or by defects in the material and therefore perform a diffusion process. At low temperatures the predominant process of the two is through conduction electrons, which depends linearly on the temperature:

$$k(T) \propto T \text{ or } k(T) = a \cdot T$$

For metals like copper, silver and aluminium the coefficient *a* can vary a lot depending on treatment and purity, the so-called residual resistivity ratio (*RRR*). This value of this *RRR* comes from the ratio of the electrical resistance at room temperature to the resistance at low temperatures, e.g. 4.2 K the boiling point of liquid helium. For copper the thermal conductivity is given by:

$$k(T) = \frac{RRR}{0.76} \cdot T \quad \left[\frac{\mathrm{W}}{\mathrm{Km}}\right]$$

Typical values for the thermal conductivity of copper at 1 K are in the range 20-1000 depending on the purity. The graph below depicts the thermal conductivity of copper for various *RRR*-values at different temperatures.

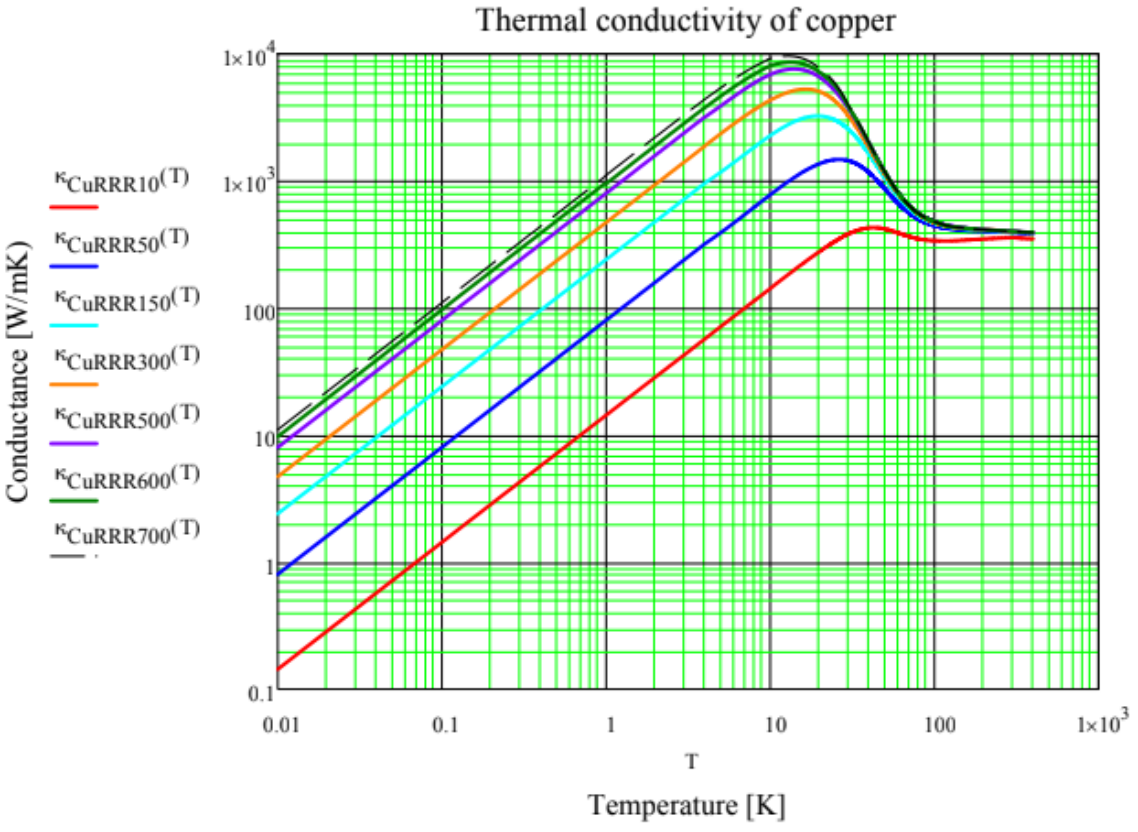

Fig. 3: Thermal conductivity of copper for various RRR-values.

2.2. Specific heat

Another material property which is dependent on temperature (at low temperatures) is the *specific heat (C)*. It is a measure of how much energy is necessary to increase the temperature of the material. Specific heat is closely related to thermal conductivity and for metals also depends on the same two processes: *conduction electrons* and *lattice vibrations.* However, contrary to the thermal conductivity, both processes play an important role at low temperature. Where conduction electrons have a linear dependence on temperature, phonons have a cubic dependence, i.e. $C \propto T^3$.

Hereto at low temperatures the specific heat can be written as:

$$C = \gamma T + \beta T^3$$

Note: "low" temperatures means "small compared to the Debye temperature" if we consider the phonons and "small compared to the Fermi temperature" if we consider the electrons. A typical value for the Fermi temperature is 10^4 K, whereas the Debye temperature for copper is 344 K.

In the figure below the specific heat of copper is depicted. The corresponding equation and variables can be found in the appendix.

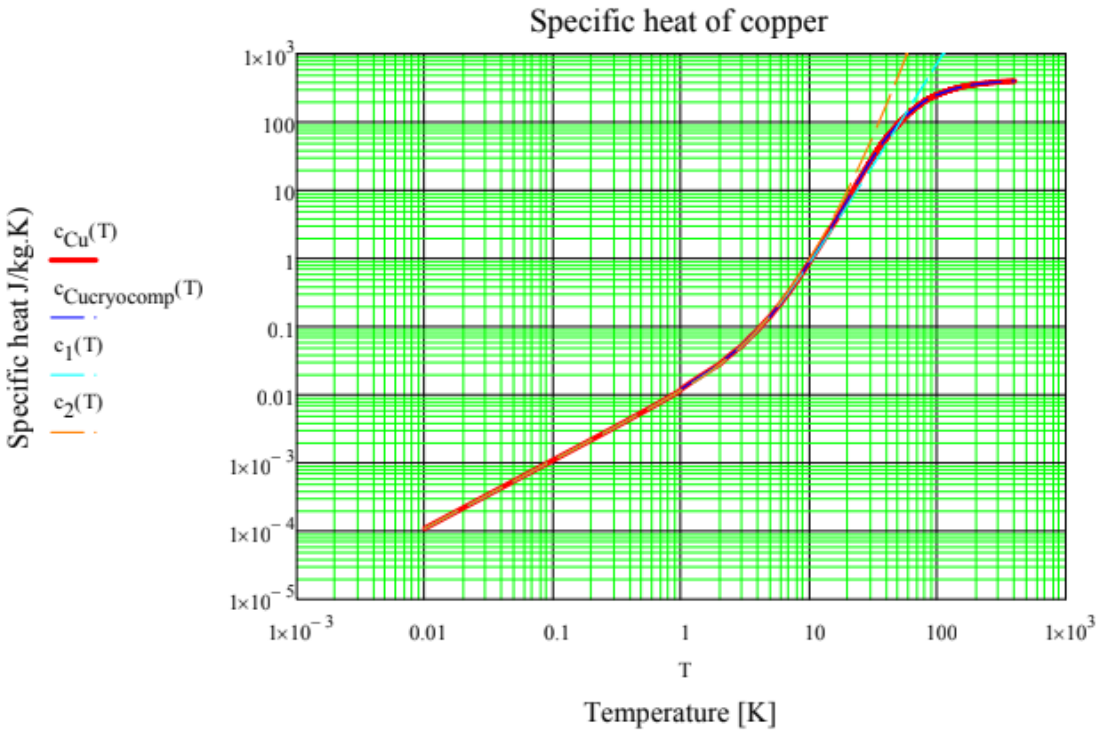

Fig. 3: Specific heat of copper according to various sources.

2.3. Contact resistance

When heat transfers from one material to another a temperature drop occurs termed the thermal contact resistance. The figure below depicts this phenomenon where x_2 denotes the interface between two surfaces in contact with each other.

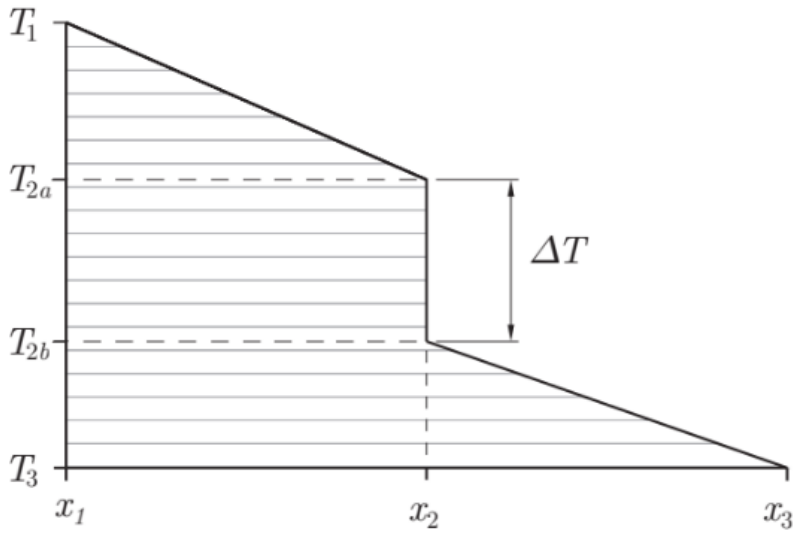

Fig. 4: Thermal contact resistance as a result of two surfaces in contact.

The contact resistance is defined as:

$$R = \frac{\Delta T}{Q} = \frac{\Delta T}{qA}$$

It is a ratio between the temperature drop, ΔT, over the interface subject to the total heat input Q (qA). The main reason for the contact resistance is that the real contact area between the two contacting materials is just a small fraction of the apparent contact area, see Figure 5. The fraction between actual and apparent area, $\frac{A-\text{real}}{A-\text{apparent}}$, depends on several parameters such as surface roughness, surface hardness and contact pressure.

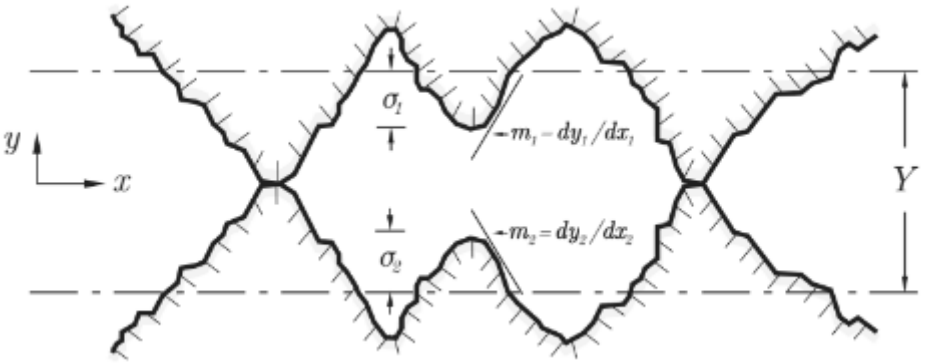

Fig. 5: Interface of two materials in contact with one another.

The joint conductance h_j is defined as the reciprocal of the resistance:

$$h_j = \frac{1}{RA} = \frac{q}{\Delta T}$$

It is comprised of three contributions: contact conductance h_c , gap conductance h_g and radiative conductance h_r. The contact conductance is the thermal conduction between the contacting surfaces. Gap conductance is the conduction that takes place through the gas-filled gaps. The last contribution, radiative conductance, is the conductance due to thermal radiation between the two materials. These contributions work in parallel and therefore the joint conductance can be written as:

$$h_j = h_c + h_g + h_r$$

As the LC-cooler is near-vacuum, the gap conductance should not play a major role. For the thermal radiation contribution, this is also negligible as we are at very low temperatures and radiation has a fourth order dependence on temperature. As such, for our setup the main contribution is due to contact conductance.

The total thermal contact conductance is given by:

$$C_c = \frac{Q}{\Delta T}$$

2.4. Heat equation

One desire is to obtain the temperature distribution in a given material, i.e. how temperature varies with position. This distribution is important as one can calculate at any point the conduction heat flux from Fourier's law. To describe the temperature distribution we use the law of energy conservation. Hereto, define the (differential) control volume as depicted below with infinitesimally dimensions dx, dy and dz.

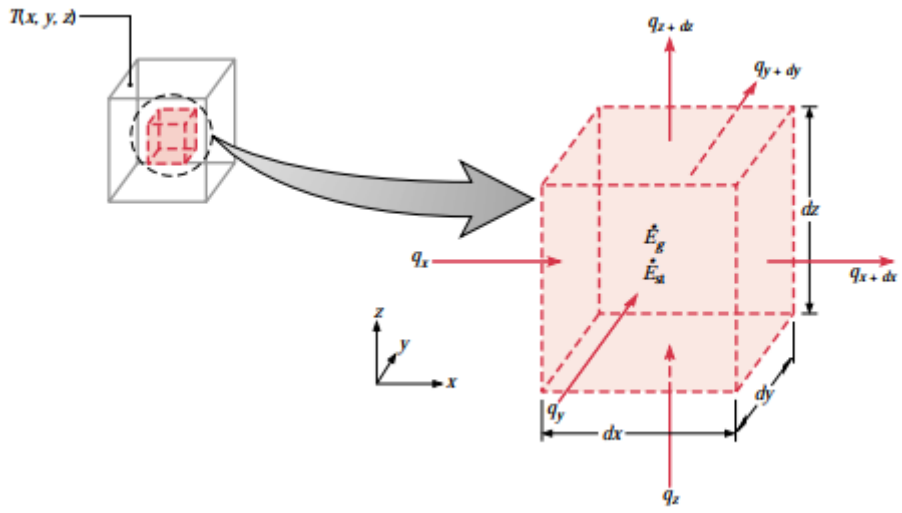

Fig. 6: Heat flow through a differential control volume dxdydz.

Heat can flow through each of the 6 surfaces able to alter the total energy stored in the system. If temperature gradients are present, heat transfer by means of conduction will take place across the

control surfaces. For each dimension the conduction can be expressed as a first order Taylor series, resulting in:

$$q_{x+dx} = q_x + \frac{\partial q_x}{\partial x} dx$$

$$q_{y+dy} = q_y + \frac{\partial q_y}{\partial y} dy$$

$$q_{z+dz} = q_z + \frac{\partial q_z}{\partial z} dz$$

For our existing setup we can neglect any energy source term, $\dot{E}_g$, which occurs due to thermal energy being converted into either chemical, electrical or nuclear energy or the other way around. The difference between in- and outflow of energy results in a change in the total energy stored in the system, $\dot{E}_{st}$. The energy storage term can be expressed as:

$$\dot{E}_{st} = \rho c_p \frac{\partial T}{\partial t} dxdydz$$

where $\rho c_p \frac{\partial T}{\partial t}$ expresses the time rate of change of thermal energy of the material per unit volume.

As a consequence of energy conservation we obtain:

$$\dot{E}_{in} - \dot{E}_{out} = \dot{E}_{st}$$

$$q_x + q_y + q_z - q_{x+dx} - q_{y+dy} - q_{z+dz} = \rho c_p \frac{\partial T}{\partial t} dxdydz$$

Substituting latter equation for the conduction expressed as a Taylor series, it follows that:

$$-\frac{\partial q_x}{\partial x} dx - \frac{\partial q_y}{\partial y} dy - \frac{\partial q_z}{\partial z} dz = \rho c_p \frac{\partial T}{\partial t} dxdydz$$

Recall that conduction follows Fourier's law:

$$q_x = -k(T) \frac{dT}{dx} dydz$$

where we use the cryogenic property that thermal conductivity is temperature dependent. Similar formulations exist for the other dimensions. As such, substituting the energy balance for Fourier's law for conduction:

$$\frac{\partial}{\partial x}\left(k(T) \frac{\partial T}{\partial x}\right) + \frac{\partial}{\partial y}\left(k(T) \frac{\partial T}{\partial y}\right) + \frac{\partial}{\partial z}\left(k(T) \frac{\partial T}{\partial z}\right) = \rho c_p \frac{\partial T}{\partial t}$$

For **one-dimensional steady-state heat flow** this formula simplifies to:

$$\frac{\partial}{\partial x}\left(k(T) \frac{\partial T}{\partial x}\right) = 0$$

2.5. Relation thermal and electrical circuit

Between thermal and electrical systems many analogies can be made. In the following table similarities between the two systems are made:

H_t Heat (Joule)	Q_t Heat flow rate (J/s)	C_t Thermal capacitance	R_t Thermal resistance	T Temp (Kelvin)	-
q Charge (Coulomb)	I Current (Ampere)	C Capacitance (Farad)	R Resistance (Ohm)	V Voltage (Volt)	L Induction (Henry)

The subscript t is being used to denote thermal systems.

Thermal capacitance is given by:

$$C_t = mC_p \text{ , with } m\text{=mass and } C_p\text{=specific heat}$$

Thermal resistance is given by:

$$R_{t,cond} \equiv \frac{T_1 - T_2}{q} = \frac{L}{kA}$$

which has an electrical analogy:

$$R_{electrical} \equiv \frac{E_1 - E_2}{I} = \frac{L}{\sigma A}$$

with E representing the electrical potential, I the current and σ the electrical conductivity. As such it is possible to represent a thermal model by an electrical circuit

Example: From thermal model towards electrical circuit.

Consider the following thermal model:

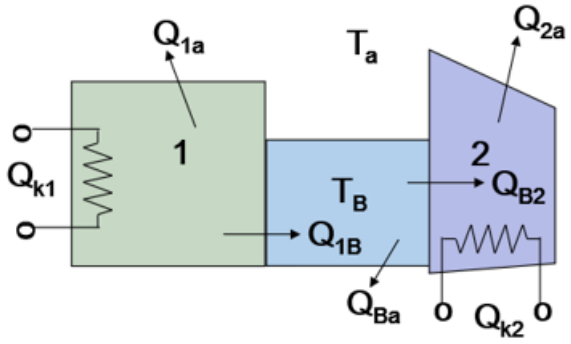

Fig. 7: Example of a thermal model.

In this model we have three separate rooms. Rooms 1 and 2 are warmed up by heaters Q_{k1} and Q_{k2}. The rooms are connected through room 3 which is kept at a constant temperature T_B. All three rooms have heat transferring to the surrounding atmosphere T_A. For the electrical equivalent model

notice that the two heaters can be represented by current sources whereas a voltage source for the constant temperature T_B. The heat transfer between rooms 1 & 2 with the atmosphere can be seen as thermal resistances. As for the warm up or cool down of the rooms 1 & 2, a transient behaviour takes place which is where thermal capacitors come into play as the internal room temperature changes with time. The resulting electrical circuit is depicted in the figure below.

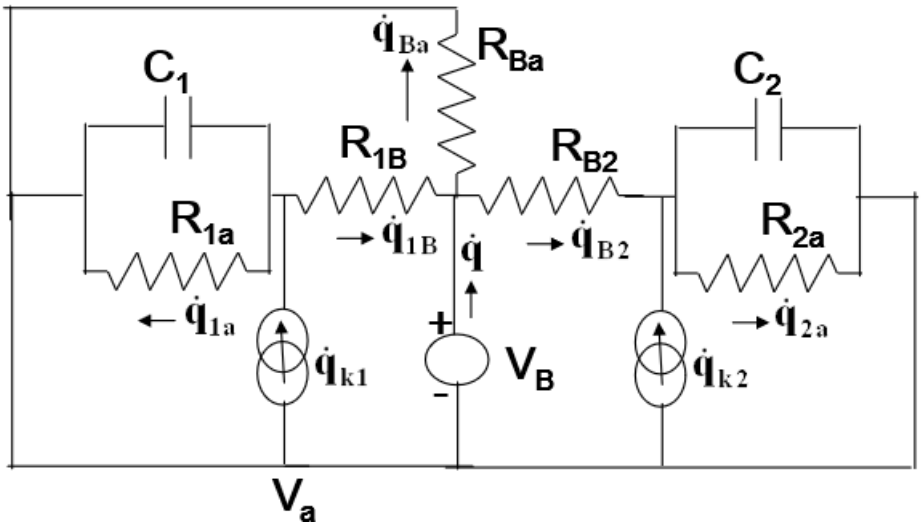

Fig. 8: Electrical circuit representation of the thermal model.

Note how the inputs of the thermal model are the heat sources Q_{k1} and Q_{k2} and the controlled temperature T_B. This translates to currents $\dot{q}_{k1}$ and $\dot{q}_{k2}$ and controlled voltage V_B as inputs for the electrical system.

3. Analysing the 700 mK strap dynamics

One major part of this internship is to understand the temperature behaviour inside the LC-cooler. An important component of this is the 700 mK stage which consists of the still plate and a copper strap attached to the plate which is illustrated in the figure below. The still plate can be interpreted as a heat sink. It is a large thermic mass capable of dispersing heat (within certain limits) while remaining fairly constant.

For all measurements that I have done over the course of the internship I investigated steady-state conditions. Recall from section 2.5 that a thermic mass has the electrical equivalence of a capacitor. For transient behaviour this capacitor analogy plays an important role for understanding the cool-down or warm-up of the strap as that is determined by RC-times. At steady-state the “capacitor” is fully charged and steady-state temperature values describe the thermal conductance of the strap.

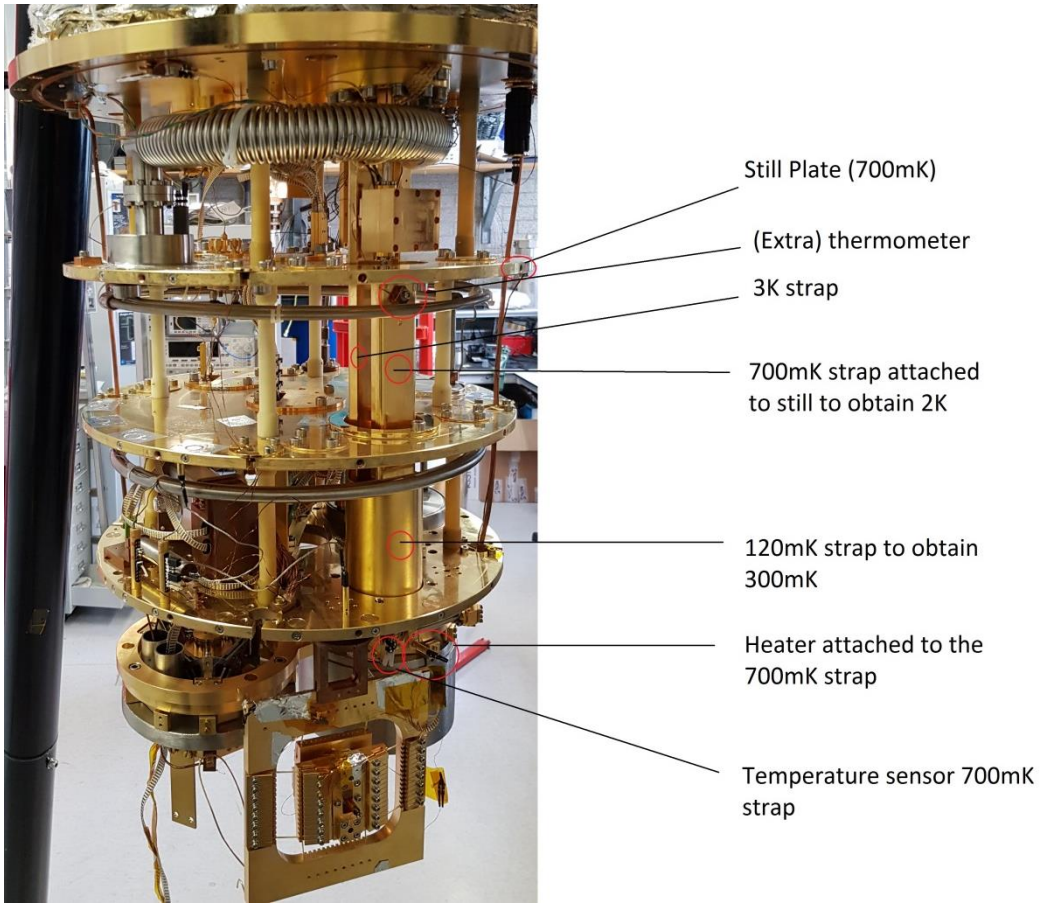

Fig. 9: 700 mK strap and accompanying instruments.

Characteristics

Object	**Length (m)**	**Surface area (m^2)**	**Mass (kg)**
Still plate	-	-	7.5
700 mK strap	0.2684	Apparent: $1.24 \cdot 10^{-4}$ Effective: $1.13 \cdot 10^{-4}$	0.253
3 K strap	0.392	Apparent: $1.16 \cdot 10^{-4}$ Effective: ?	0.388

3.1. First measurement (done on 8th of February)

On the 8th of February I started doing my first measurements on the 700 mK strap's dynamics. To get a grasp of the mechanics at play I investigated several input values for the heater placed at the end of the strap. See the table below for steady-state values.

I/P Finger (mA/mW)	***T_{still} (mK)***	***T_{finger} (mK)***	***Condition***
0/0	656	745	Steady-state
7/4.9	823	2808	Steady-state
5/2.5	740	2090	Steady-state

Note that there exists a temperature gradient at steady-state even though the heater at the strap's end is turned off. This is odd as one would expect to have the same temperature for the still and strap upon having no external power to the system. A possible reason for this might be in the location of the still's thermometer. It is placed on top of the still where still a dynamic process is happening between the different temperature levels and hence might differ from the still's actual temperature, i.e. a temperature of 745 mK same as the strap. As such, we presume a temperature off-set in the still's temperature which we check for the second measurement (section 3.2).

However, we first assume that the obtained data is correct and from this data we will calculate the strap's thermal conductance and RC-times.

3.1.1. Strap's thermal conductance

In this section the thermal properties of the strap will be examined. It is assumed that the strap's *RRR* should be around 500 since it has undergone a heat treatment. This means that around 1 K the thermal conductivity is given by:

$$k(T) = 798 \cdot T \left[\frac{\mathrm{W}}{\mathrm{mK}}\right]$$

For arbitrary *RRR*-values of copper the thermal conductivity around 1 K is given by:

$$k(T) = a \cdot T \left[\frac{\mathrm{W}}{\mathrm{mK}}\right], \text{ with } a = \frac{RRR}{0.76}.$$

Moreover, recall the one-dimensional steady-state heat equation from section 2.4:

$$\frac{\partial}{\partial x}\left(k(T)\frac{\partial T}{\partial x}\right) = 0$$

This equation is useful as it allows us to determine the steady-state temperature distribution in the strap by means of separation of variables:

$$\frac{\partial}{\partial x}\left(k(T)\frac{\partial T}{\partial x}\right) = \frac{\partial}{\partial x}\left(a \cdot T\ \frac{\partial T}{\partial x}\right) = 0$$

$$a \cdot T\frac{\partial T}{\partial x} = constant = C_1,$$

which, in integral form, is given by:

$$\int k(T)dT = \int a \cdot TdT = \int C_1 dx = C_1 x + \ C_2$$

$$a\frac{T(x)^2}{2} = C_1 x + C_2$$

where $C_1 = \frac{a(T_2^2 - T_1^2)}{2L}$ and $C_2 = \frac{a}{2}T_1^2$. The values T_1 and T_2 denote respectively the temperature at the strap's end (heater-side) and strap's start (still-side).

Hence, the **strap's temperature function** at steady-state is given by:

$$T(x) = \sqrt{\frac{T_2^2 - T_1^2}{L}x + T_1^2}$$

Below the temperature distribution is illustrated for the case where the strap's end is heated up to 2.8 K by applying 4.9 mW.

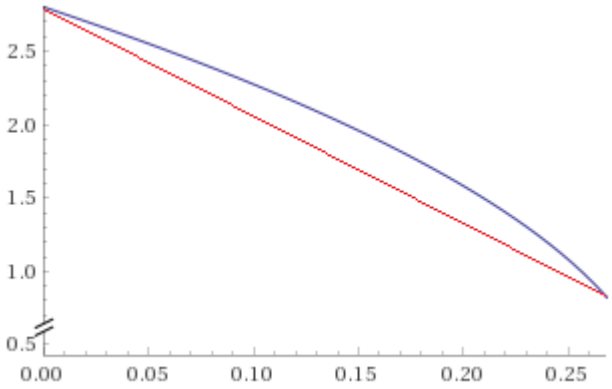

Fig. 10: Temperature distribution for the strap with T_1=2.8 K and T_2=0.8 K. Blue = temperature distribution due to linear temperature dependence of the thermal conductivity. Red = temperature distribution due to constant thermal conductivity. The vertical axis depicts kelvins, whereas the horizontal axis is the length of the strap.

A point of interest is whether the obtained temperature gradient is consistent with the applied power. To investigate this we make use of Fourier's law for heat conduction. Hence, recall:

$$q = -k(T)A\frac{dT}{dx}$$

Again, making use of separation of variables and that the heat rate is a constant at steady-state:

$$\int_0^L q\,dx = A\int_{T_1}^{T_2} -k(T)\,dT = A\,\lambda_{Cu}(T_2, T_1)$$

$$q = \frac{A}{L}\,\lambda_{Cu}(T_2, T_1) = \frac{A}{L}\left(a\frac{T_1^2 - T_2^2}{2}\right)$$

Let us first assume an *RRR*-value of 500 for the strap, which means that the thermal conductivity is:

$$k(T) = 798 \cdot T\left[\frac{\mathrm{W}}{\mathrm{mK}}\right]$$

Upon applying **no external power (P_{Finger}=0)** the steady-state heat flow becomes:

$$q = \frac{A}{L}\,\lambda_{Cu}(667, 750) = 4.2 \cdot 10^{-4}\left(\frac{798}{2}(0.75^2 - 0.667^2)\right) = 19.7\mathrm{mW}$$

This result immediately raises questions as the supposed heat flow is a lot larger than zero, the expected outcome, and the maximum applied power (4.9 mW). However, with the current *RRR,* what would the expected temperature be at the strap's end for P_{finger}=4.9 mW?

$$4.9 \cdot 10^{-3} = 4.2 \cdot 10^{-4}\left(\frac{798}{2}(T_1^2 - 0.823^2)\right)$$

$$T_1^2 = \frac{2}{798} \cdot 11.67 + 0.823^2$$

$$T_1 = 0.840K$$

As such, an increase of only a few millikelvins would be expected. This raises the question how large the heat rate actually needs to be to obtain the temperature gradient from 0.823 K to 2.808 K we currently measure:

$$q = \frac{A}{L}\,\lambda_{Cu}(823, 2808) = 4.2 \cdot 10^{-4}\left(\frac{798}{2}(2.808^2 - 0.823^2)\right) = 1.21\text{W}$$

Likewise for the temperature gradient from 0.740 K to 2.090 K:

$$q = \frac{A}{L}\,\lambda_{Cu}(667, 750) = 4.2 \cdot 10^{-4}\left(\frac{798}{2}(2.09^2 - 0.740^2)\right) = 0.64\text{ W}$$

Note that the total heat flow roughly decreased by a factor 2 by going from 4.9 mW to 2.5 mW applied power. As such the applied power does scale linearly with the calculated heat flows, which is to be expected.

However, for both temperature gradients we observe a much larger heat flow than one would assume, namely 4.9 mW and 2.5 mW. There exist a couple of possibilities as to why this is the case. The first one being that the contact resistances play a large role. Since only two thermometers are being used for the current setup – one at the top of the still plate and the other at the strap's end (heater side) – we cannot directly measure the contact resistance between the still plate and the strap's start (still-side). It could be the case that the contact resistance is responsible for a big heat drop, whereas the strap itself shows the presumed behaviour, i.e. an increase of a few millikelvins across the beginning and end point of the strap. A second possibility is that the strap's conductance is worse than presumed. Even though the strap did undergo a heat treatment the material's quality is lacking. These two possibilities will be examined during the second measurement [see also section 3.2]. The third possibility could be that the thermometer is directly being heated up by the heater as they are located next to each other. This is the least likely of the three possibilities as the thermometer can only be heated up through radiation. Since radiation follows a fourth order temperature dependence this effect should be minimal at cryogenic temperatures. However, to rule the effect out, this possibility is investigated during the third measurement series [see section 3.3].

3.1.2. RC-times

It is important to get a sense of the RC-times that are at play as the temperature regulation is directly linked to it. If the sample rate for instance is slower than the RC-time, the temperature control is always running behind. Typically the sample rate for many temperature control systems is in the range 2-5 seconds. The question arises whether this holds true at low temperature. As a rule of thumb the sample rate should be 5-10 times faster than the RC-time of the system [5].

This housekeeping computer with which we control the LC-cooler's temperature behaviour has a sample time of about 30 seconds. This means that every 30 seconds one data point is collected. For our first measurement the heater was set to apply the strap with 4.9 mW. The strap's end resulted in being heated up to 2.8 K, after which the heater was turned off and the cool down was being

monitored [see Figure 11]. The RC-time is acquired by the amount of time it takes for the heated material to cool down to 36.8% of the maximum present temperature.

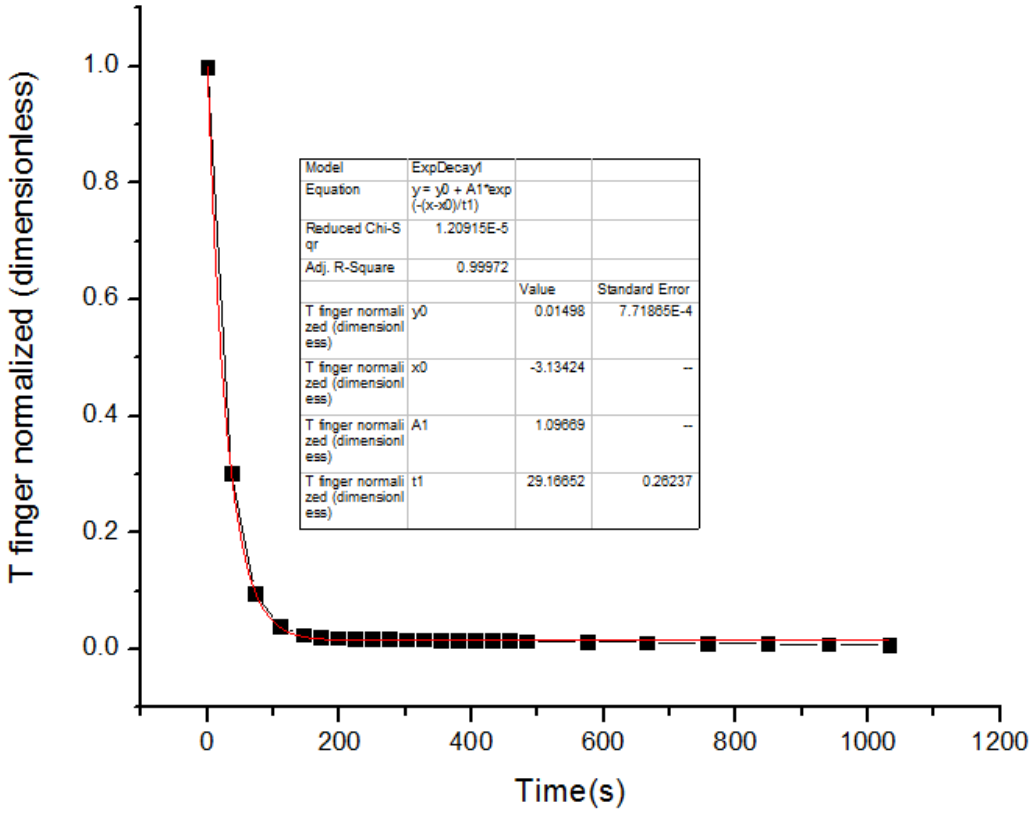

Fig. 11: Normalized cool down strap after being heated up to 2.8 K.

The cool down of the strap in Figure 11 has been normalized to better compare the cool down processes at different temperatures. Moreover, the RC-time is easier to read from the plots. As a first estimate a fit has been made through the data which uses an exponential decay function. The fit that was assigned estimated an RC-time of about 29 seconds. To see if the fit being used is sufficient enough or that multiple RC-times are at play the log-plot of the data was examined. Straight lines on the log-plot translate to exponential functions in a normal plot. Looking at log-plot depicted in Figure 12, we clearly notice two segments which can be fitted by a straight line. This translates to two RC-times being present in the cool down process.

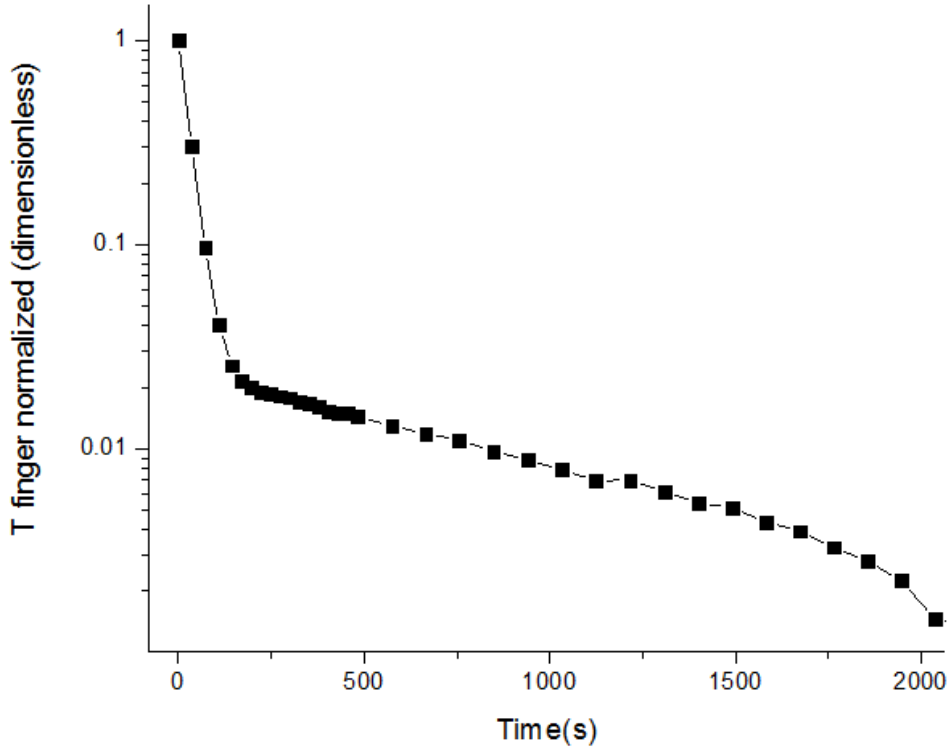

Fig. 12: Log-plot cool down strap from 2.8 K.

Knowing that there are two RC-times occurring in the strap's cool down, the fit with only one exponential function isn't sufficient to completely describe the process. As such, Figure 13 displays two different fits for the process. One is where the whole domain is being used via the equation:

$$y = A_1 e^{-x/t_1} + A_2 e^{-x/t_2} + y_0$$

where t_1 and t_2 denote the RC-times and y_0 is the slight off-set with the x-axis.

The other method is where the domain is split up in two parts to only account for the straight lines in the log-plot and dismissing the curve connecting these straight lines. As such, for each part of the domain the data is fitted with a normal exponential fit:

$$y_1 = A_1 e^{-x/t_1} + y_0$$
$$y_2 = A_2 e^{-x/t_2} + y_0$$

Again the RC-times are obtained from the value for $t_1$and t_2 and y_0 the slight off-set with the horizontal axis. As a result the RC-time of approximately 29 seconds is measured once more, but moreover a longer RC-time of 1000 seconds is observed. As our sample time is 30 seconds we cannot rule out the possibility that faster RC-times have been "missed". Hereto, we plan to sample as fast as possible for the next measurement series to see if this is the case.

In section 3.2.4 the RC-times will be investigated in more detail and compared to theoretical values. In this section multiple cool downs at different temperature levels are included.

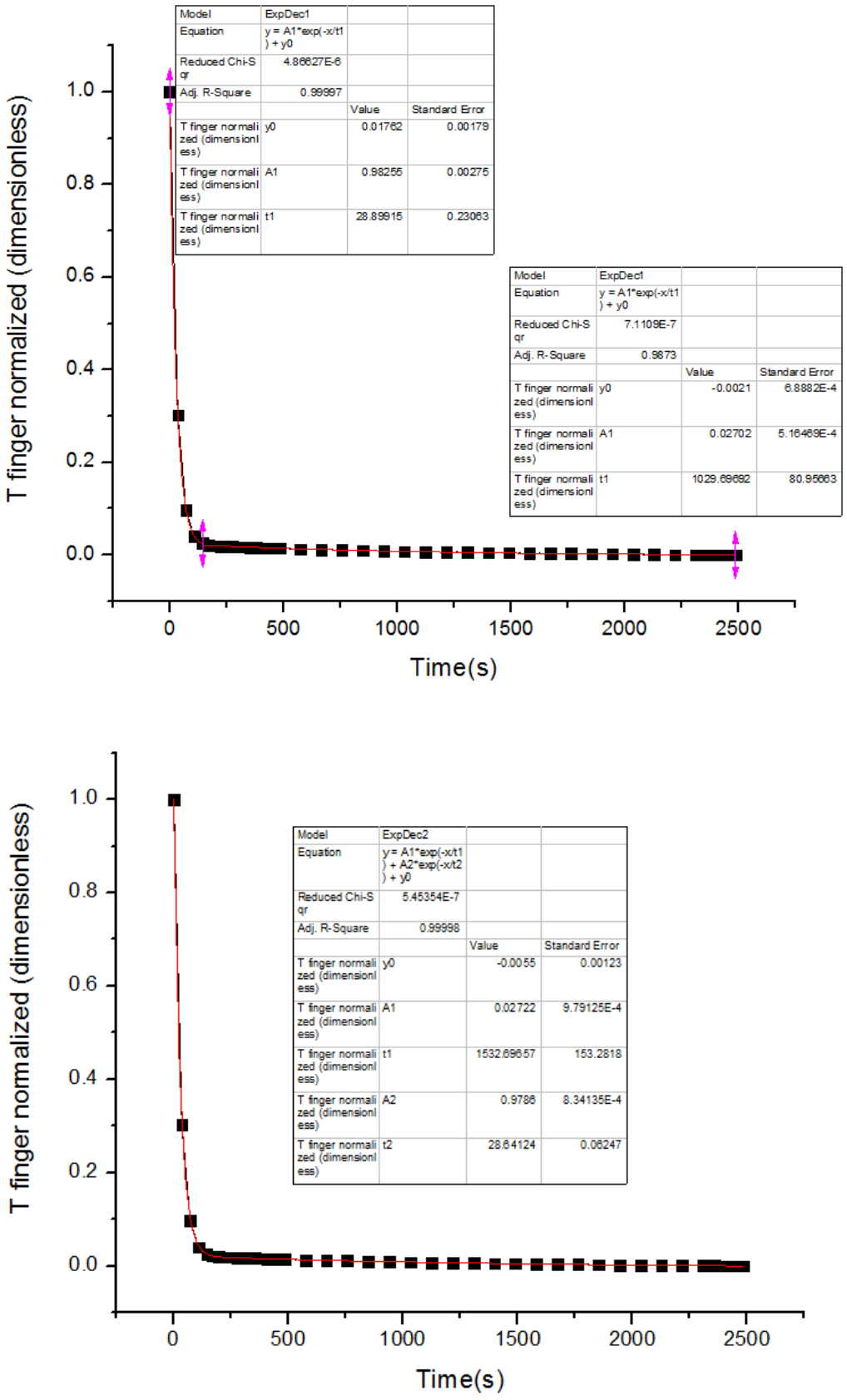

Fig. 13: Top: one exponential fit per domain (split in two). Bottom: the whole domain fitted by two exponential functions.

3.2. Second measurement (done on 2nd and 3rd of March)

For the second measurement some changes have been made to the existing setup [discussed in 3.2.1]. Moreover, by separately monitoring a single output we can improve the sample rate to obtain **one data point every second**. Increasing the sample rate any further is not possible with the existing setup. Hence, if any, faster RC-times than a second will not be noticed from the obtained data. In section 3.2.2. we discuss and implement a strategy such that the still's temperature does not alter too much upon different power supplies to the heater. The later sections contain information on the strap's thermal dynamics such as: thermal conductance, RC-times and contact resistances.

3.2.1. Changes made to the existing setup

As the setup was not able to separately give the thermal dynamics of the strap and the still, conclusions were hard to draw as many effects were not able to be examined properly, e.g. the contact resistance between the still plate and the 700 mK strap. Hereto, some changes have been made:

- Added thermometer on the still plate to directly measure the still's temperature.
- Added thermometer on the strap's still-side to measure any contact resistances and directly measure the strap's thermal properties.
- Two heaters were used simultaneously this time, namely one on the still plate and the existing one at the end of the strap.

3.2.2. Dynamic heating

A dynamic heating process has been chosen in order to not put too much load on the still. The total applied power was kept constant, such that the still temperature would not fluctuate too much (+-20mK). Previously set of measurements allowed a total temperature change of 150 mK (i.e 20-25% of the still's normal temperature) to take place over the still. With the help of two heaters (still and strap) a power of 4.9 mW was kept constant. One heater was placed at the top of the still, whereas the other at the strap's end. The table below shows the input values of the current for both the still and the end of the strap.

Measurement state	Still current (mA)	Strap current (mA)	Total power (mW)
1	7	0	4.9
2	6.7	2	4.9
3	4.9	5	4.9
4	3.6	6	4.9
5	0	7	4.9

Table 1: Measurement's set

Looking at table above, if we were to be in state 1 we would go to state 2 by lowering the still current by 0.3 mA and apply a strap current of 2 mA immediately after to once again obtain 4.9 mW of total power applied to the system.

Our measurements consisted of going from state 1 to 5 (warm-up process of strap) and then to go from state 5 back to state 1 (cool-down process of strap). One channel (e.g. the end of the strap) was measured on a different computer on which a faster sample rate could be achieved while the others were monitored on the housekeeping computer.

3.2.3. Strap's thermal conductance

As we now have two thermometers at both end points of the strap we are now in the position to properly determine the strap's thermal properties. But before venturing into that topic let us first examine the steady state values of the still and the strap when no power has been applied to the system.

Steady-state: No external power (P_{heater}=0)

T_{still}≈561.6 mK
$T_{strap\text{-}still\ end}$= T_1=648.9/649.23 mK
$T_{strap\text{-}heater\ end}$= T_2=648.3/648.2 mK

For steady-state the above mentioned numbers should be equal to each other. We can observe that for steady-state **both strap measurement points (T_1 and T_2)** give the same result with **an acceptable error (+-1 mK).** As such, we can assume both temperature sensors are most likely to be properly calibrated.

However, the still temperature seems to have an offset as it is "nowhere" near the strap temperature. A possibility for this skewed number is that it is measured at the top of the still where a continuous dynamic process is taking place. One wants to measure this temperature as it acts as an indicator whether or not the process is operating within bounds. However, the temperature measured at this moment, i.e. on the top of the still, could differ from the actual still temperature. We also installed a thermometer on the still plate itself, yet no improvement could be obtained as the thermometer wasn't properly calibrated. Hence, for future measurements, the hypothesis of a temperature offset should be confirmed.

If we assume **the still temperature** to have the same value as the **strap**, a **temperature offset** of **87.3 mK** has to be accounted for. For all results in the upcoming sections this offset has been added to the measured still's temperature.

Steady-state heat flow through the strap

In order to determine the thermal conductivity of the 700 mK strap multiple power inputs at steady-state have been examined also known as the measurement states. An overview of this can be seen in Table 2 which furthermore depicts the power of the heater and the heat flow one would expect with a strap's *RRR* of 700.

Measurement state	T_1 (mK)	T_2 (mK)	Predicted/ measured heat flow (mW)
1	*816*	*789*	*-*
2	*910*	*1068*	*0.4 / 52*
3	*1184*	*2060*	*2.5 / 476*
4	*1299*	*2400*	*3.6 / 682*
5	*1439*	*2744*	*4.9 / 914*

Table 2: Steady-state values for various power inputs (measurement states)

As one can tell from the table above, factors up to 190 difference between predicted and actual heat flow are measured. Recall from section 3.1.1. that we listed 3 possibilities for the big difference between predicted and measured heat flow, namely: contact resistance, strap's thermal conductance is poor or heater warms up the thermometer by means of radiation. Since the measurements are done purely on the strap itself, we can rule out contact resistance. As for radiation effects this will be discussed in section 3.3.1 since we shielded both thermometer and heater for the third measurement. If we assume that the measured temperature gradient is correct due to the strap's poor thermal conductance we are able to calculate the thermal conductivity by:

$$q = \frac{A}{L}\,\lambda_{Cu}(T_2, T_1) = \frac{A}{L}\left(a\frac{T_2^2 - T_1^2}{2}\right)$$

where $a = \frac{RRR}{0.76}$. With $\frac{A}{L} = 4.2 \cdot 10^{-4}$ and for $q = 4.9$ mW, $T_1 = 1439$ mK and $T_2 = 2744$ mK we can calculate the *adjusted thermal conductivity*:

$$k(T) = a \cdot T = 2\frac{L}{A}\frac{q}{T_2^2 - T_1^2} \cdot T = 4.3 \cdot T\left[\frac{\mathrm{W}}{\mathrm{mK}}\right]$$

and an *RRR* of roughly 3, which is much lower than the presumed *RRR* of 500.

Possibilities why the strap could be this bad:

- Material is not pure enough
- The annealing treatment has not been done correctly

In section 4 we will investigate the *RRR*-values in more detail.

3.2.4. RC-times

In section 3.1.2. it became apparent why RC-times are important as they provide an indication for the sample rate that one needs to use. As such we will investigate the RC-times that are at play in the dynamical system in more detail at various temperature levels. We mainly focus on RC-times of the strap's end (heater-side), T_2, as the data provides more accurate representations because the temperature values are not as close to the still temperature as T_1. In the appendix graphs of the RC-times of T_1 are displayed.

Determining RC-times of T_2

First off we will examine the case where, after heating the strap's end to 2.8 K, we let it cool down by 350 mK through dynamic heating. Hence, the still temperature remains roughly stable. In section 3.1.2 we have seen that, aside from 1300s for the dynamical behaviour of the system, an RC-time of roughly 30 seconds was visible. However, due to the sample rate of 30s, we couldn't see RC-times faster than this. In the figure below the strap's thermal data has been plotted with a single exponential fit. If no other RC-times are present, the fit should properly line-up with the data and give an RC-time of 30s.

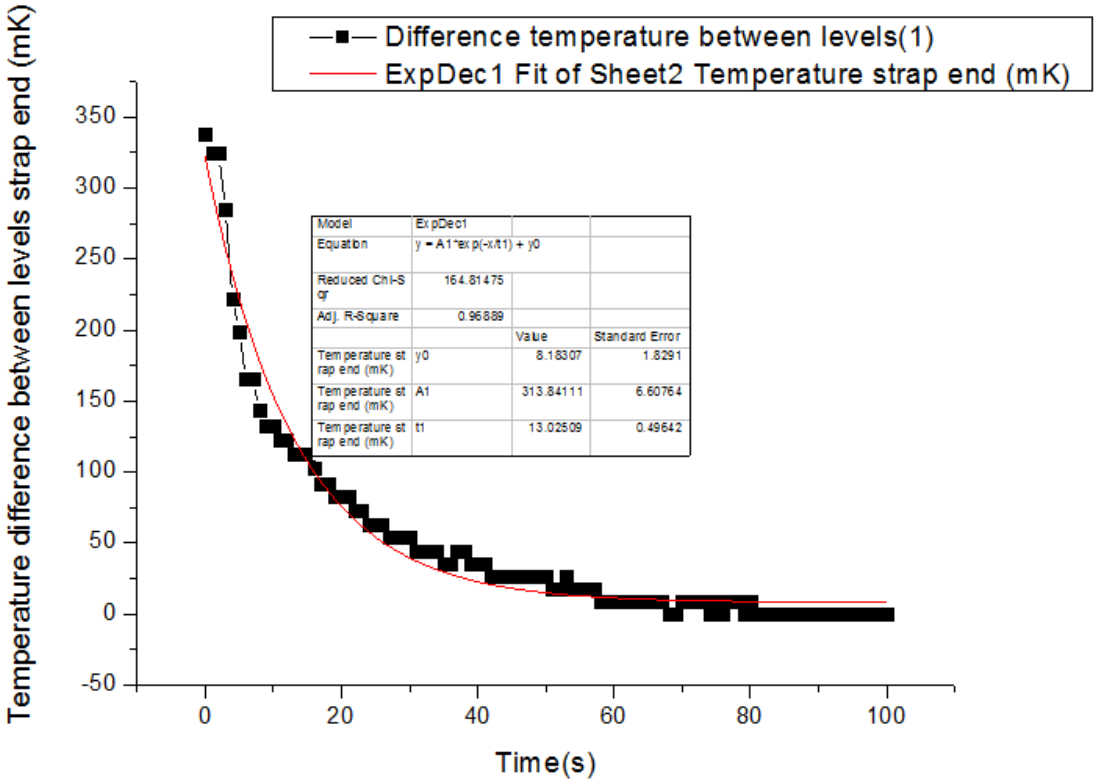

Fig. 14: Raw data cool down from 2.8 K fitted with a single exponential fit.

As can be seen from Figure 14 the fit does not represent the raw data that well. The fit results in an RC-time of 13s which indicates that faster RC-times are part of the equation. As such, from the log-plot of the raw data (Figure 15) two RC-times are visible. Hereto, the data has been fitted by two exponential functions which retrieves the **29.0 ± 3.7s RC-time** from section 3.1.2, but moreover makes a much faster **RC-time** visible of **5.0 ± 0.6 seconds**. One of these should be related to the strap while the other RC-time should be the characteristic of the still. As the RC-time has a theoretical background (R denotes the (thermal) resistance while C denotes the (thermal) capacity) one can also predict beforehand the outcome of the RC-times. We will discuss this later on in this section.

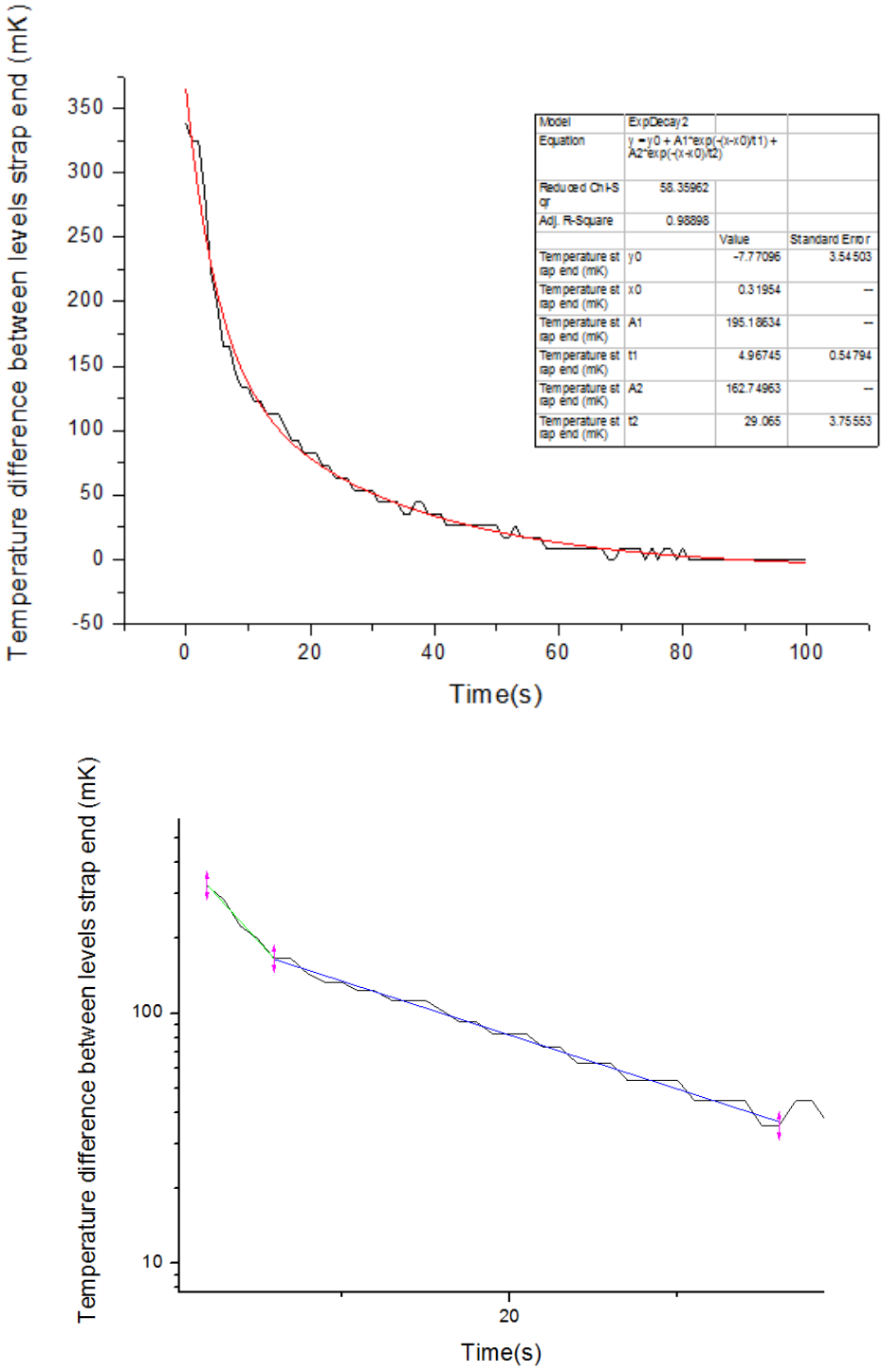

Fig. 15: Top: Data fitted with two exponential functions. Bottom: Log-plot making 2 RC-times visible.

Recall from section 2.1.1 how thermal resistance (R_t) is related to thermal conductivity:

$$R_{t,cond} \equiv \frac{T_1 - T_2}{q} = \frac{L}{kA}$$

As we have that the thermal conductivity is temperature dependent we also have R_t to be temperature dependent. Hereto, the product *RC* becomes dependent on the temperature. To illustrate this phenomenon two other cool downs at different temperatures have been examined,

see Figure 16. For the top one the strap underwent a cool down from 6 mA to 5 mA (3.6 mW to 2.5 mW). **RC-times of 22.7 ± 0.6 s and 2.3 ± 0.1 s** are measured. The graph at the bottom depicts the cool down from 5 mA to 2 mA (2.5 mW to 0.4 mW) which results in **RC-times of 27.1 ± 0.7 s and 2.7 ± 0.1 s** being measured.

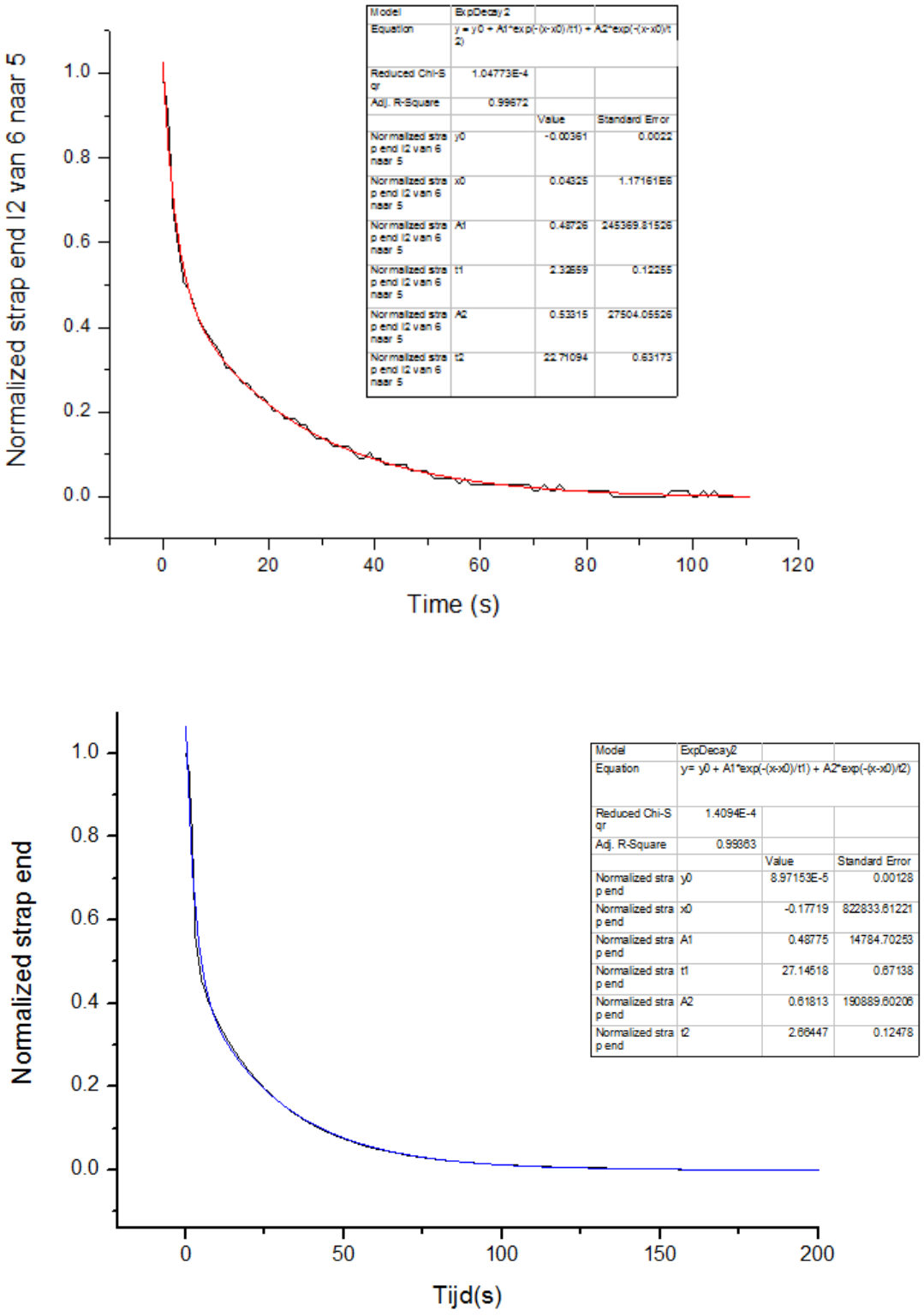

Fig. 16: Top: Cool down 3.6 mW to 2.5 mW. Bottom: Cool down 2.5 mW to 0.04 mW.

Theoretical RC-time

We can also calculate the RC-time and see if our expectations are close to measured outcomes.

Strap:

If we consider the 2.8 K cool down we observe a temperature gradient of 1300 mK upon applying 4.9 mW power. Hereto, the thermal resistance becomes:

$$R_{t,cond} \equiv \frac{T_1 - T_2}{q} = \frac{1.3\ \mathrm{K}}{4.9\ \mathrm{mW}} = 265\ \mathrm{K/W}$$

As for the thermal capacitance $C_t = mC_p$ we have m=0.253 kg and C_p=0.03 J/kg K (for pure copper) at 2.0 K (average temperature). Thus:

$$C_t = mC_p \approx 0.0075\ \mathrm{J/K}$$

A list of all the RC-times at different temperatures can be found in the table below:

Temperature strap's end	$R_{t,cond}$	C_t	$R_{t,cond}C_t$ / RC
2.8 K (4.9 mW)	265	0.0075	2 s / 5 s
2.4 K (3.6 mW)	303	0.00625	1.9 s / 2.3 s
2.0 K (2.5 mW)	360	0.005	1.8 s / 2.7 s

Table 3: Theoretical versus experimental RC-times.

The theoretical RC-time values are close to the measured values. The small offset could be explained by the fact that the temperature does not linearly decrease across the strap at steady-state, which is the assumption for the calculation of the thermal resistance. Moreover, it is not clear whether or not the thermal capacitance depends on the *RRR*-value.

Still plate:

Upon determining the thermal capacitance of the still plate we have a much larger thermic mass: 7 kg. As the still plate is kept a (roughly) constant temperature (0.86 K) the specific heat can be assumed to be:

C_p=0.01 J/kg K, and thus $C_t = mC_p \approx 0.07$ J/K

As for the thermal resistance it is a bit unclear what contributions are present. If we only assume contact resistance is the contributor we have $\boldsymbol{R_t}$**=120 K/W** (value obtained from section 3.2.5). As such an **RC-time of 8 seconds** would be expected for the still. If we assume the strap's thermal resistance is an addition to the total thermal resistance of the still we would obtain:

$$R_{t,still} = R_{t,strap} + R_{contact}$$

$R_{t,strap}$	$R_{contact}$	$RC - time$
265	120	26.6 s
303	120	29.4 s
360	120	33.6 s

Note: even though these values are in the region of expectation, we cannot say the contributions are correct. Since the strap seems to be worse than expected this also has consequences for the specific heat as the values used are values for pure copper.

3.2.5. Contact resistances

From the steady-state temperature values of the states mentioned in **Table 2** an estimate of the contact resistance can be made. Recall from section 2.3 the following formula to calculate contact resistances:

$$R_{cont} = \frac{\Delta T}{Q}$$

Here ΔT denotes the temperature drop from the still plate to the strap. Furthermore, Q denotes the total heatflux. As the still is kept at a constant temperature by active heating the heatflux is obtained from the applied power to the strap's heater.

In the table below the contact resistances are determined at various temperature levels for the still-side of the strap, while keeping the still plate temperature fairly constant. Moreover, we determined the contact resistance for two transitions, i.e. warm-up and cool down. As we end up in the same state we should not expect a difference in the outcome of the measured contact resistance. A difference is only observed for the transitions 1→2 & 3→2. However, this can be explained as we are close to the equilibrium of the still plate such that deviations in the temperature value are amplified.

From **Table 4** we can observe that the **contact resistance** is in the **range 100-120 K/W**. This internship only consisted of giving absolute values for the contact resistance. Whether the contact resistance is temperature dependent was beyond the scope of this project to investigate.

State Transition **(a=warm-up & b=cool-down)**	**Contact resistance still-strap**
a) 1→2	$\frac{\Delta T}{Q} = \frac{897 - 860.5}{0.4} = 90\ \mathrm{K/W}$
b) 3→2	$\frac{\Delta T}{Q} = \frac{904 - 863}{0.4} = 102.5\ \mathrm{K/W}$
a) 2→3	$\frac{\Delta T}{Q} = \frac{1162 - 861}{2.5} = 120\ \mathrm{K/W}$
b) 4→3	$\frac{\Delta T}{Q} = \frac{1162 - 865}{2.5} = 119\ \mathrm{K/W}$
a) 3→4	$\frac{\Delta T}{Q} = \frac{1268 - 862}{3.6} = 113\ \mathrm{K/W}$
b) 5→4	$\frac{\Delta T}{Q} = \frac{1268 - 865}{3.6} = 112\ \mathrm{K/W}$
a) 4→5	$\frac{\Delta T}{Q} = \frac{1386 - 866}{4.9} = 106\ \mathrm{K/W}$

Table 4: Contact resistance at different strap (still-side) temperatures.

3.3. Third measurement (done on 15th of March)

During the final measurement on the strap's dynamics we wanted to be sure that all possibilities for the strap's thermal conductance has been covered. As such, the choice has been made to shield both thermometer and heater to prevent the heater from indirectly warming up the thermometer. This effect should in principle not be a dominant force to reckon with as this can only happen by means of radiation which is a fourth order dependence of temperature. However, just to be certain, we want to rule out the possibility that this effect is present.

3.3.1. Result of shielding the thermometers and heaters

Upon shielding both thermometer and heater we performed the final experiment. The results were clear. No change in the values obtained during the second measurements was observed. As such, we can conclude that radiation did not take a part in the strap's thermal conductance which means the reason for the high temperature gradient is due to the strap's poor material. In the next section we will investigate the material in more detail and determine the *RRR*- values of the strap and various other materials.

4. Determining the *RRR* of the 700mK copper strap

One way to check whether the material being considered has the right thermal conductivity properties is by means of a **Residual-Resistance Ratio** (***RRR***) measurement. The *RRR* value (for copper) is linked linearly to the thermal conductivity. To determine the *RRR* two references are ref, namely the electrical resistance at room temperature and at 0K (or 4.2K as estimate) :

$$RRR = \frac{\rho_{300K}}{\rho_{0K}}$$

In this formula, ρ denotes the **electrical resistance** at a given temperature which is calculated by the following formula:

$$\rho = R\frac{A}{L} = \frac{U}{I}\frac{A}{L}$$

Here *I* represent the applied current through the material and *U* is the measured voltage over the material's length. The electrical resistance is a material property which means that it should not depend on the dimensions of the material, whereas the resistance *R* does.

The way we measure the resistance of a given material is by means of a **4-points measurement** ("vierpuntsmeting" in Dutch)**.** This method allows to properly determine the resistance since effects like contact resistances do not affect the outcome of the measurement. In order to measure the material's characteristics at 4.2K a dipstick is being used (see pictures below) which is placed inside a helium vessel.

Fig. 17: Left: zoomed-in version of dipstick's end; the tested material is placed between 4 points. Right: total dipstick which is used to measure resistance at 4.2K.

4.1. Current strap inside LC-cooler

The current strap inside the LC-cooler is claimed to be of pure copper which has been annealed and gold-plated. Annealing is a heat treatment that removes any defects present in the material to obtain better thermal conductivity. As a result, RRR-values of around 500 would be expected after annealing [1]. As the strap is fixed in the cooler we cannot measure the resistance at 0 K (4.2 K), however we can measure the resistance at room temperature through a 4-points measurement.

At **room temperature** a current of **6 A** has been applied through the strap and the following voltage drops were measured across the strap:

Voltage	*Measured where?*
0 µV	On the still plate itself
52 µV	Where strap is mounted to still (het "lipje")
84 µV	Next to upper thermometer
227 µV	Middle of the strap
445 µV	End of the strap
540 µV	Measured directly on the heater

Looking purely at the dynamics of the strap itself we measure a **voltage change from 85 µV to 445 µV** over a length of L=0.26m and area A=1.24·10^{-4}m^2.

As such, the electrical resistance becomes:

$$\rho_{300K} = R\frac{A}{L} = \frac{U}{I}\frac{A}{L} = \frac{445-84\ \mu\text{V}}{6\ A}\ \frac{1.24\cdot10^{-4}\ \text{m}^2}{0.26\ \text{m}} = 2.87\cdot10^{-8}\ \text{m/S}$$

And the reciprocal σ, i.e. **electrical conductance**:

$$\sigma_{300K} = \frac{1}{\rho_{300K}} = 3.48\cdot10^{7}\ \text{S/m}$$

From **Wikipedia** and **Comsol** the electrical conductivity of copper should lie between **5.96-5.99·10^7 S/m** and **annealed copper 5.80·10^7 S/m** [2]**.** This raises suspicion whether the copper strap is truly made from the presumed material.

As mentioned before, to determine the *RRR*-value a second reference point at 4.2K is needed. However, it is not desired to have the mounted strap inside the cooler be taken out anytime soon. Fortunately, in SRON's workshop, leftover material of the strap is present. This material is however raw and untreated, i.e. no heat treatment or gold-plated, but is still able to present us with insights and a worst case scenario for the strap's *RRR*-value. Next section treats this "dummy strap".

4.1.1. Dummy strap

Untreated

In this section the worst case *RRR*-value of the 700mK strap will be determined. A picture of the untreated dummy strap can be found below. Information about the strap's dimensions can be found in the Appendix.

Fig. 18: Dummy strap containing 4 holes for mounting the strap on the dipstick.

Using the 4-points measurement, at room temperature a current of 2.2A was applied and a voltage of 226 ± 2 µV was measured. Hence:

$$R_{300K} = \frac{U}{I} = \frac{226\ \mu\text{V}}{2.2\ A} = 102.7\ \mu\Omega$$

and for the electrical resistivity and conductivity:

$$\rho_{300K} = R\frac{A}{L} = 102.7 \cdot 10^{-6} * 2.3 \cdot 10^{-4} = 2.36 \cdot 10^{-8}\ \text{m/S}$$

$$\sigma_{300K} = \frac{1}{\rho_{300K}} = 4.23 \cdot 10^{7}\ \text{S/m}$$

For ρ_{0K}, the copper dummy has been dipped into a helium vessel and cooled down to 4.2 K as a best estimate. Upon applying a current of 5.102 A, a voltage between 120 and 127 µV has been measured. Hence, one obtains the following resistance:

$$R_{0K} = \frac{U}{I} = \frac{125\ \mu\text{V}}{5.1\ A} = 24.5\ \mu\Omega$$

From this, the *RRR* of the copper dummy can already be determined, namely:

$$RRR = \frac{\rho_{300K}}{\rho_{0K}} = \frac{R_{300K}\frac{A}{L}}{R_{0K}\frac{A}{L}} = \frac{R_{300K}}{R_{0K}} = \frac{102.7\mu\Omega}{24.5\mu\Omega} \approx 4.2$$

"*The typical RRR of a piece of copper which one can buy from a shop is in the range of 50-100. Heating the copper to a temperature of 400-500 °C anneals structural lattice defects, and the RRR usually increases to a value of 300-400.*" - F. Pobell, Matter and Methods at Low temperature. p.77

Annealed

For the annealed copper strap we repeat the measurements done for the untreated strap. The annealing has been done by Norma, a company located in Drachten. Below the result of the heat treatment can be seen and a log-file can be found in the Appendix.

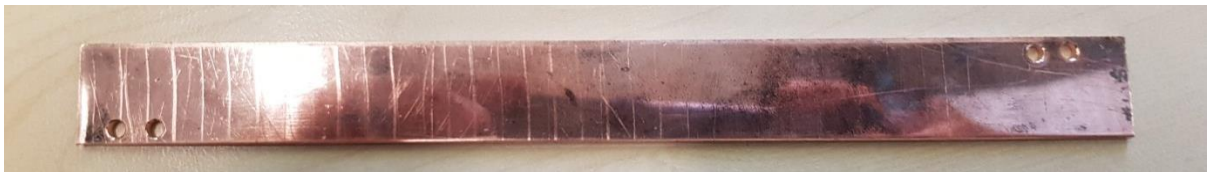

Fig. 19: Annealed copper dummy.

Like before, making use of the 4-points measurement a current of 2.275 A was applied and a voltage of 227 ± 2 µV was obtained. Hence:

$$R_{300K} = \frac{U}{I} = \frac{227\mu V}{2.275A} = 100\mu\Omega$$

For R_{0K}, we will once again dip the copper dummy into a helium vessel and let it cool down to 4.2 K. At 4.910A we measured a voltage of around 121 (+-2) µV. Hence the resistance becomes:

$$R_{0K} = \frac{U}{I} = \frac{121\mu V}{4.910A} = 24.6\mu\Omega$$

The *RRR*-value for the annealed copper strap thus results in:

$$RRR = \frac{R_{300K}}{R_{0K}} = \frac{100\mu\Omega}{24.6\mu\Omega} \approx 4.1$$

As the *RRR*-values of the copper dummy strap before and after heat treatment are almost identical, we can conclude that the treatment did not have an impact on our "copper" strap. A reason for this might be that the strap did not consist purely of copper. For pure copper, annealing should increase the *RRR*-value. To test this presumption we also investigate the resistances of other "known" materials in the next section.

4.2.Other materials

Results from the copper dummy strap suggest that the material conducts poorly. Before a decision is being made whether or not to replace the 700 mK strap, we also tested different materials to support this theory which are displayed in the following table:

Material	Room temperature	Helium vessel (4.2 K)	*RRR*-value
Silver-plated copper wire with a nickel-layer	Current: 3.911 A Voltage: 3900 µV	Current: 4.930 A Voltage: 38 µV	130
Gold-plated copper wire	Current: 4.600 A Voltage: 5590 µV	Current: 4.650 A Voltage: 80 µV	70

The *RRR*-values of these materials are much closer to what literature predicts. Hereto, it seems that the 700 mK strap is from a different material than was presumed.

4.3. New strap "ECu-57"

As a result of the poor conductance through the present 700 mK strap, new material (see Fig. 20) has been ordered, namely copper: **"ECu-57"**. The material characteristics can be found in the Appendix. Like the current 700 mK strap, this newly ordered strap needs to be annealed and gold-plated. All processes combined, this can take a couple of weeks before fully finished. As we want to confirm that the poor conductance is caused by the strap inside the cooler, two gold-plated copper wires will be placed parallel to the 700 mK strap at the next time the LC-cooler is warm again.

Fig. 20: From top to bottom; untreated strap, annealed strap and new "ECu-57" strap.

In the table below one can find the thermal properties of the new material. Note: With the current set-up we could not reach a higher accuracy than 1 µV. Hereto, a factor 2 uncertainty is present.

Material	Room temperature	Helium vessel (4.2 K)	*RRR*-value
ECu-57	Current: 4.400 A Voltage: 332 µV	Current: 6.062 A Voltage: 1-2 µV	225 - 450

One should be aware that the strap's *RRR*-value is before any heat treatment. So far this is the best *RRR*-value obtained of any measured material. After heat treatment it is expected that the value increases up to 700.

5. Results parallel wire to 700 mK strap

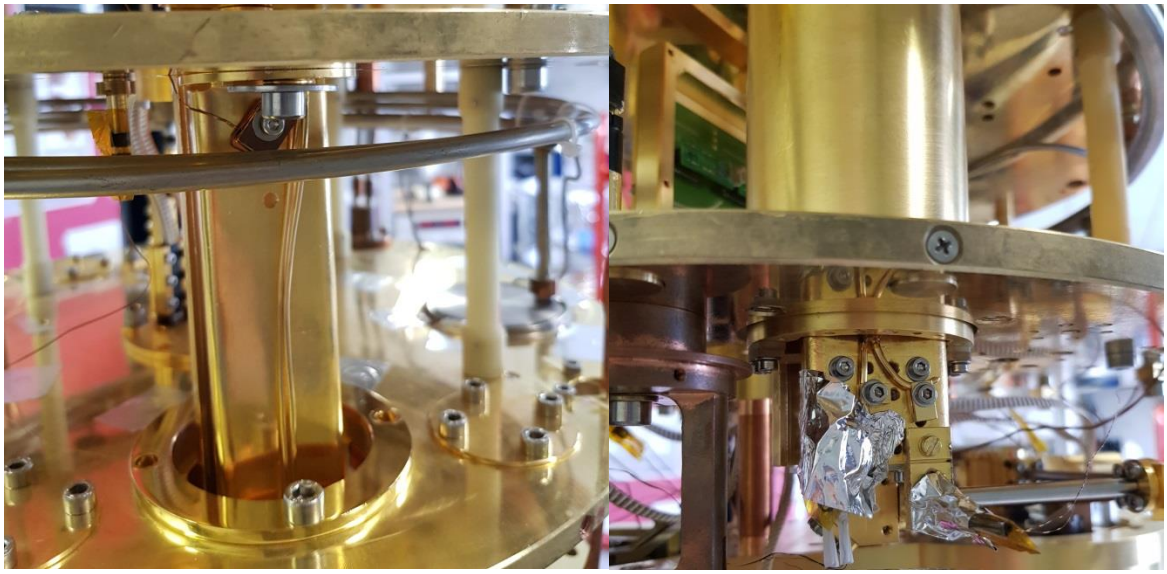

Fig. 21: Two thermal straps placed parallel to the strap.
Note also the shielding on thermometer and heater.

To immediately confirm that the strap is worse than expected we place two gold-plated copper wires (*RRR* of 70) parallel to the 700 mK strap. As the wires should be responsible for most of the heat transfer we expect a noticeable change in the temperature gradient, namely roughly half of what we previously measured. During the cool down after the instalment, we noticed that the wires were responsible for a thermal short circuit. As such, we weren't able to cool down properly and as the time for my internship ran short, I wasn't able to confirm my hypothesis with the newly placed thermal wires.

6. COMSOL

In this section the cool down of the entire strap has been examined using the software program COMSOL. This piece of software allows the user to investigate heat flows through various types of materials and geometries. In our case we limited ourselves to a simple geometry, i.e. a one-dimensional bar. The strap at the still-side was kept at a constant, however the heater's side we raised the temperature to 2.8 K. Hence, to be at the temperature level obtained from the setup upon applying 4.9 mW to the strap's end (heater-side). The figure below illustrates the cool down process at various timestamps. If we assume the strap to be of the previously presumed material, i.e. having an *RRR* of 500, the whole strap would be in its equilibrium state after just 0.03s. However, following the results from the *RRR*-value determination the strap reaches steady-state after 3 seconds. Recalling the RC-times results from section 3.2.4. this value is in the range of what we

measured. Hence, this further solidifies the presumption that the strap is not of the material one first expected.

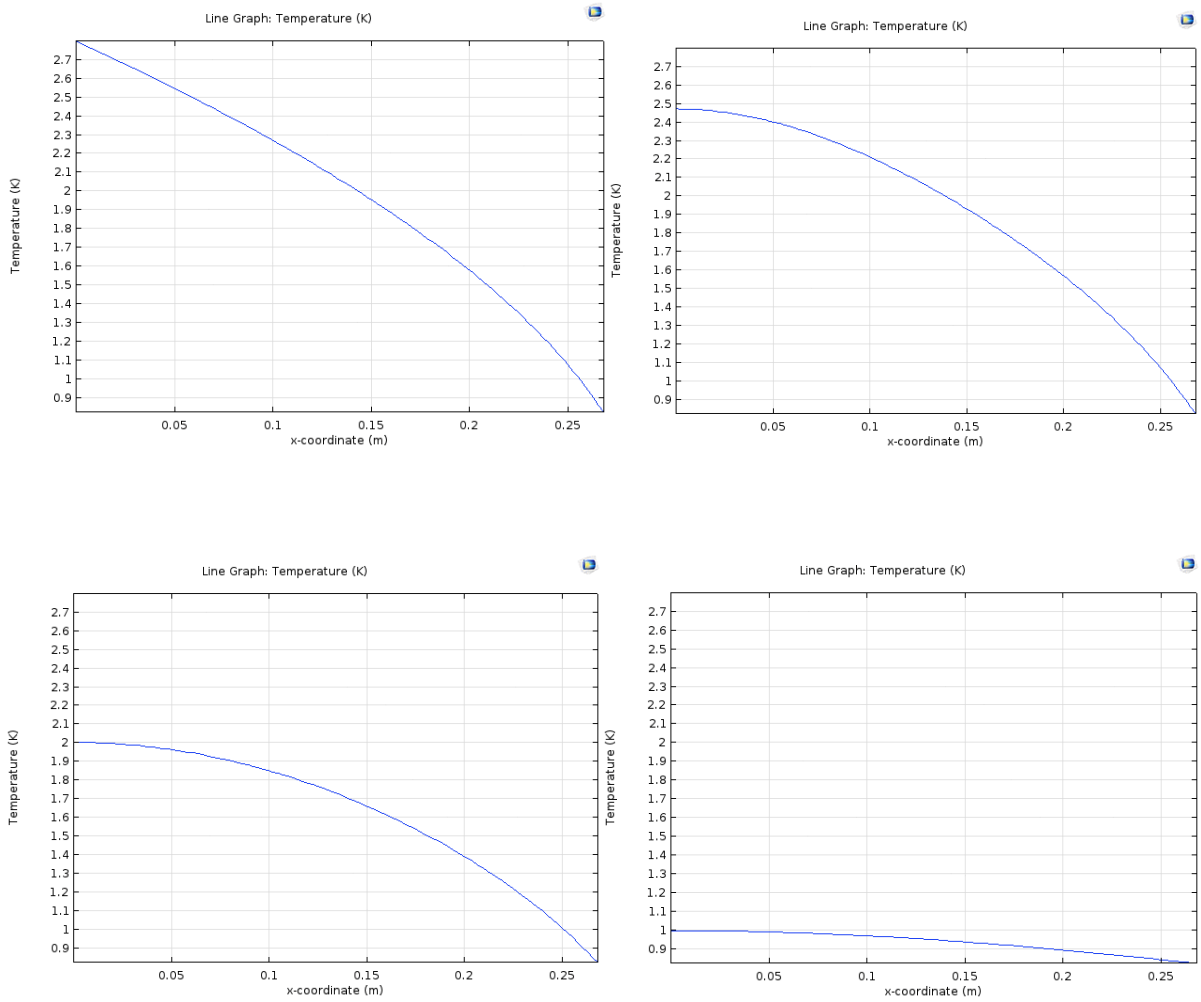

Fig. 21: Cool down strap at various times using COMSOL.

7. Discussion

Since analysing the thermal behaviour took way longer than anticipated the original assignment of temperature control was hardly touched. However, in this section I want to state some points which are useful for future research on the thermal model. As the thermal conductivity is temperature dependent one has a non-linear temperature distribution across the strap. Hereto, one cannot simply model the temperature gradient by a single thermistor (thermal resistor) as this only works for linear temperature gradients. Therefore, one needs to discretise the strap into multiple pieces such that each piece approximately has a linear temperature gradient and hence can be expressed by a thermistor. So for the whole strap multiple thermistors need to be used.

As we hardly touched thermal modelling I included a Q&A with Henk van Weers about the thermal model of the DM-FPA in the Appendix. I hope this can act as a starting point towards modelling and control of the LC-cooler's thermal behaviour.

Another point of discussion is the thermal capacitance. In section 2.2 the specific heat was investigated, although we did not/could not investigate whether the specific heat depends on the *RRR*-value of the material. Moreover, since calculation in this report have been done assuming the thermal capacitance to be that of pure copper the outcomes can be a bit skewed as the material did not turn out to be pure copper.

8. Conclusions & Advice

During this internship I primarily investigated the thermal behaviour of the 700 mK strap inside the LC-cooler (Leiden Cryogenics). A high temperature gradient was soon to be apparent. From all possible reasons, we could rule out contact resistance and radiation to be the cause of this temperature gradient after follow-up measurements. This left us with thermal conduction as the reason which depends on *k*, the thermal conductivity, a characteristic of the material. At cryogenic temperatures (<50 K) this material property becomes temperature dependent. It was presumed that the strap's thermal conductivity was $k(T)=798 \cdot T$. The coefficient is dependent on the material's purity, which is measured by the *RRR*-value (Residual- Resistance Ratio). An *RRR*-value of 500 is needed to obtain the strap's thermal conductivity, which is considered to be high quality. After various measurements on the strap's thermal properties it turned out that the 700 mK (and 3K) strap are of different material than first assumed. Calculating the *RRR*-value of the strap using a 4-points measurement an *RRR*-value of 4.2 was obtained. The process of finding the cause of the huge temperature gradient was very time consuming as people were certain the material was of the assumed quality. Hence, an advice would be to first properly determine and document the quality of the material used for the set-up.

For future research:

- Investigating thermal dependence of the 3 temperature levels.
- Constructing a thermal model of the LC-cooler.
- Connecting it to the existing thermal model of the DM-FPA.

As it is important to not overload the still plate its temperature needs to be fairly constant. Making use of a dynamic heat process where the total power input is a constant this can be obtained. As such I advise to implement this for the temperature control of the system.

9. References

[1] F. Pobell, *Matter and Methods at Low Temperatures,* 1992

[2] Wikipedia, https://en.wikipedia.org/wiki/Electrical_resistivity_and_conductivity, consulted February 2018

[3] T.L. Bergman & F.P. Incropera, *Fundamentals of Heat and Mass Transfer*, 7th edition, 2011

[4] Thermal modelling, *http://slideplayer.com/slide/3387404*, consulted February 2018

[5] Control Station, *https://controlstation.com/sample-rate-needed-tuning-pid-controllers/*, consulted February 2018

10. Appendix

10.1. Specific heat formula

Specific heat of Copper

$g\_atom_{Cu} := 63.57 \cdot 10^{-3} \frac{kg}{mol}$

$\Theta_{01copper} := 345.8K$

$\Theta_{02copper} := 347.7K$

$\gamma_{copper1} := 165.2 \cdot 10^{-3} \frac{cal}{K^2 \cdot mol}$ $\gamma_{copper1} = 0.69166 \cdot \frac{J}{mol \cdot K^2}$

$\gamma_{copper2} := 165.3 \cdot 10^{-3} \frac{cal}{K^2 \cdot mol}$

$H_{copper} := 0 \cdot 10^{-3} cal \cdot \frac{K}{mol}$

$B := 0.02 \cdot 10^{-3} \frac{cal}{K^6 \cdot mol}$

$$c_1(T) := \frac{H_{copper} \cdot T^{-2} + \gamma_{copper1} \cdot T + \left[\frac{464.34 \cdot \left(\frac{cal \cdot 10^3}{mol \cdot K} \right)}{\left(\Theta_{01copper} \right)^3} \right] \cdot T^3}{g\_atom_{Cu} \cdot 10^3}$$

$c_1(1K) = 2.77536 \times 10^{-3} \frac{mol}{kg} \cdot \frac{ca}{mo}$

$$c_2(T) := \frac{\left[\left(H_{copper} \cdot T^{-2} \right) + \gamma_{copper2} \cdot T + \left[\frac{464.34 \cdot \left(\frac{cal \cdot 10^3}{mol \cdot K} \right)}{\left(\Theta_{02copper} \right)^3} \right] \cdot T^3 + B \cdot T^5 \right]}{g\_atom_{Cu} \cdot 10^3}$$

$$c_{Cu}(T) := \begin{cases} \text{linterp}\left(P_{Cu}, R_{Cu}, \frac{T}{K} \right) \cdot \frac{J}{kg \cdot K} & \text{if } 1K < T \le 400K \\ 10^{\alpha\left(\frac{T}{K}, N_{Cu} \right)} \cdot \frac{J}{kg \cdot K} & \text{if } 1K \le T \le 1K \\ \dfrac{\left[\left(H_{copper} \cdot T^{-2} \right) + \gamma_{copper2} \cdot T + \left[\frac{464.34 \cdot 10^3 \cdot \left(\frac{cal}{mol \cdot K} \right)}{\left(\Theta_{02copper} \right)^3} \right] \cdot T^3 + B \cdot T^5 \right]}{g\_atom_{Cu} \cdot 10^3} & \text{if } 0K < T \le 1K \end{cases}$$

(2 Cryocomp

(1 Nist

(6,11 Pobell and Kaplan&Glass

$$c_{Cucryocomp}(T) := \begin{cases} \text{linterp}\left(P_{Cu}, R_{Cu}, \frac{T}{K} \right) \cdot \frac{J}{kg \cdot K} & \text{if } 1K < T \le 400K \\ 0 \quad \text{otherwise} \end{cases}$$

10.2. Dimensions straps

Dimension	Strap untreated	Strap annealed
Length (mm) -Total -Outer holes (from center) -Inner holes (from center)	 195 mm 177 mm 162 mm	 196 mm 177 mm 162 mm
Width (mm)	18,68 mm	18,68 mm
Depth (mm)	2 mm	2 mm

10.3. Strap's still-side RC-times

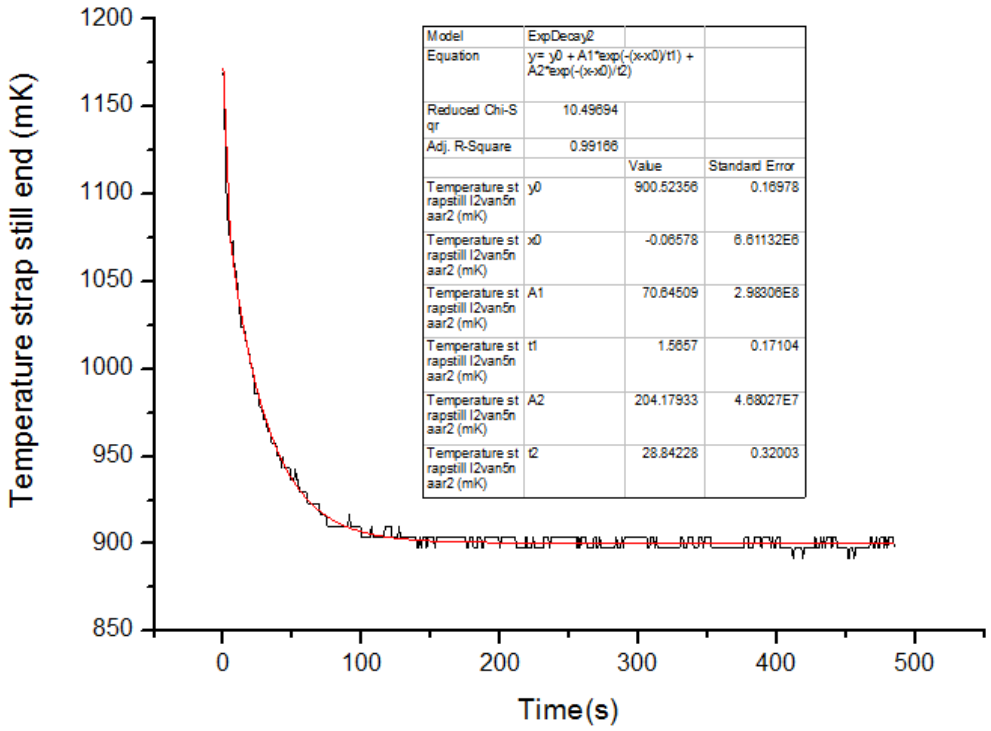

Appendix Fig. 1: Cool down from 1.2 K to 0.9 K. t_1 and t_2 denote the RC-times.

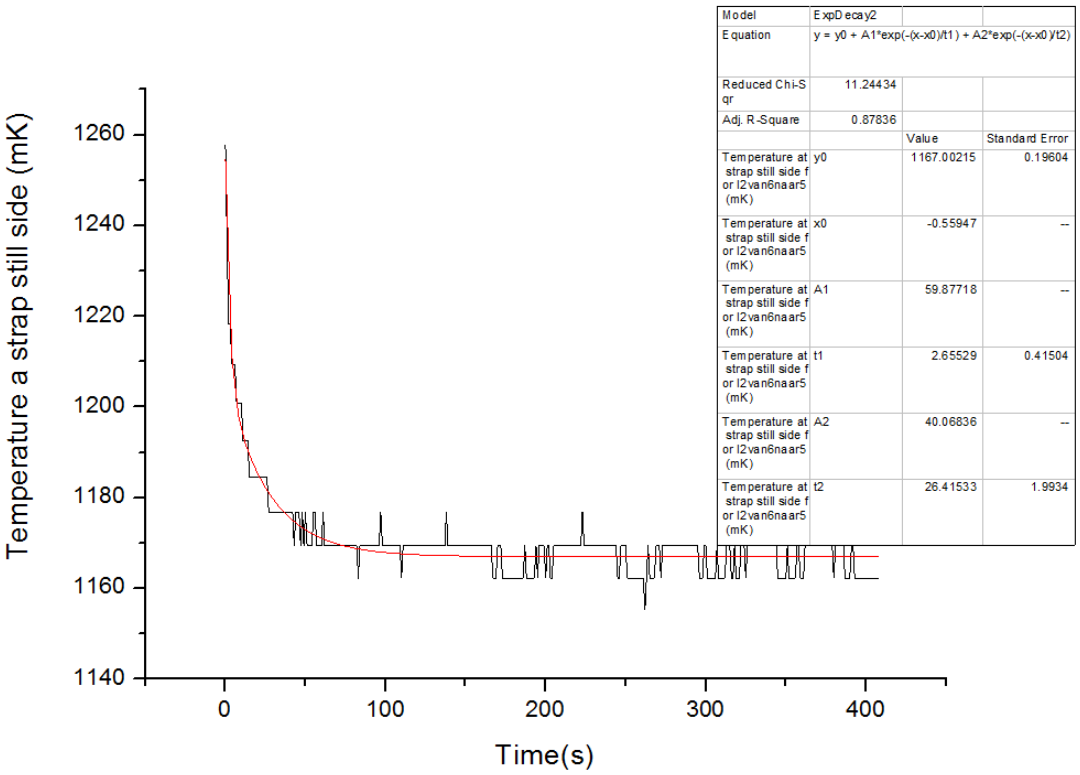

Model	ExpDecay2		
Equation	y = y0 + A1*exp(-(x-x0)/t1) + A2*exp(-(x-x0)/t2)		
Reduced Chi-Sqr	11.24434		
Adj. R-Square	0.87836		
		Value	Standard Error
Temperature at strap still side for l2van6naar5 (mK)	y0	1167.00215	0.19604
Temperature at strap still side for l2van6naar5 (mK)	x0	-0.55947	--
Temperature at strap still side for l2van6naar5 (mK)	A1	59.87718	--
Temperature at strap still side for l2van6naar5 (mK)	t1	2.65529	0.41504
Temperature at strap still side for l2van6naar5 (mK)	A2	40.06836	--
Temperature at strap still side for l2van6naar5 (mK)	t2	26.41533	1.9934

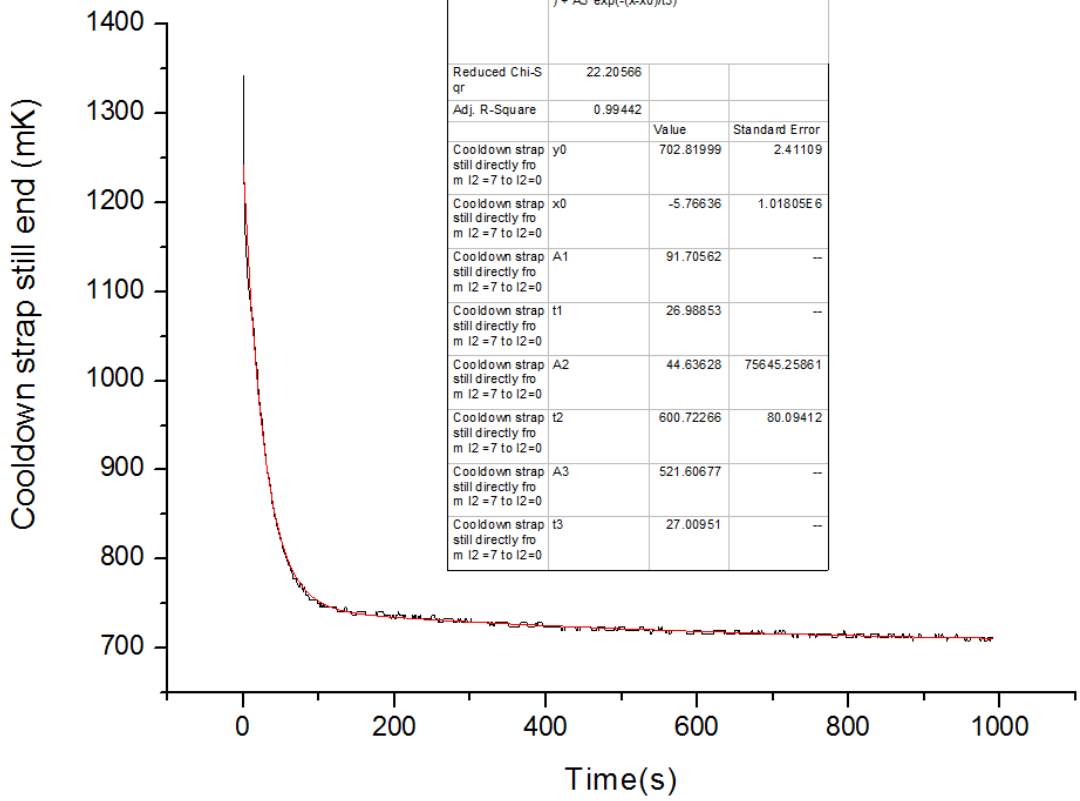

Model	ExpDecay3		
Equation	y = y0 + A1*exp(-(x-x0)/t1) + A2*exp(-(x-x0)/t2) + A3*exp(-(x-x0)/t3)		
Reduced Chi-Sqr	22.20566		
Adj. R-Square	0.99442		
		Value	Standard Error
Cooldown strap still directly from l2=7 to l2=0	y0	702.81999	2.41109
Cooldown strap still directly from l2=7 to l2=0	x0	-5.76636	1.01805E6
Cooldown strap still directly from l2=7 to l2=0	A1	91.70562	--
Cooldown strap still directly from l2=7 to l2=0	t1	26.98853	--
Cooldown strap still directly from l2=7 to l2=0	A2	44.63628	75645.25861
Cooldown strap still directly from l2=7 to l2=0	t2	600.72266	80.09412
Cooldown strap still directly from l2=7 to l2=0	A3	521.60677	--
Cooldown strap still directly from l2=7 to l2=0	t3	27.00951	--

Appendix Fig. 2: Top: Cool down from 1260 mK to 1170 mK. Bottom: Cool down to the still plate temperature, 3 RC-times are present.

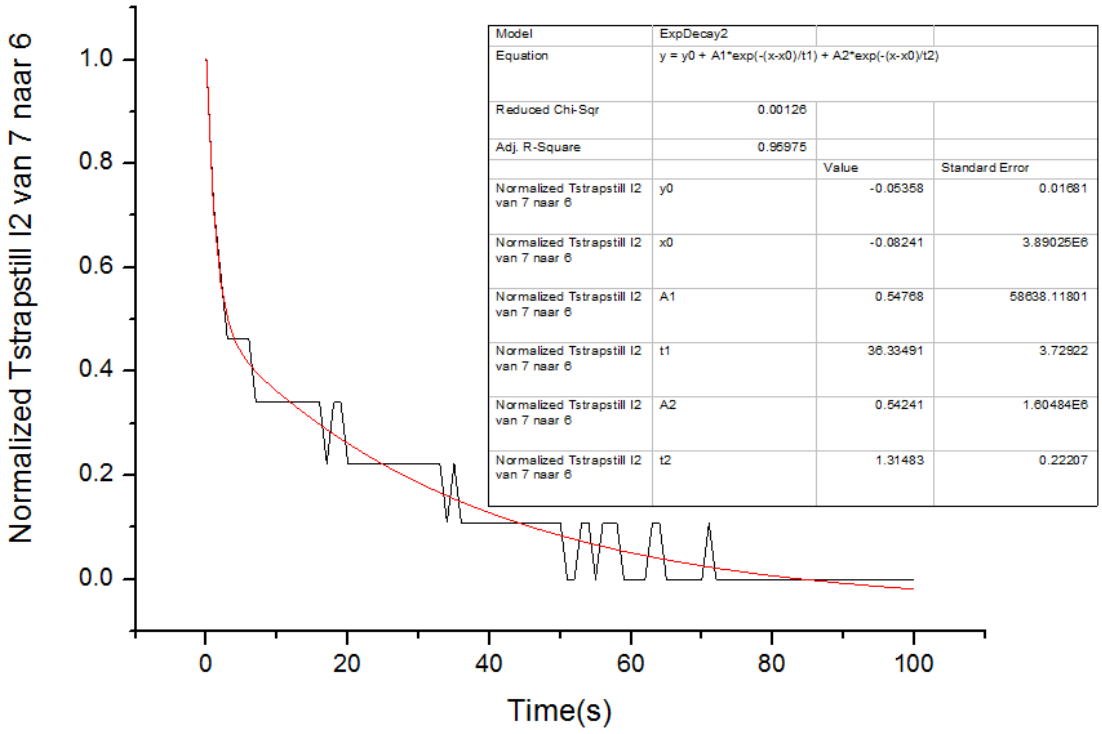

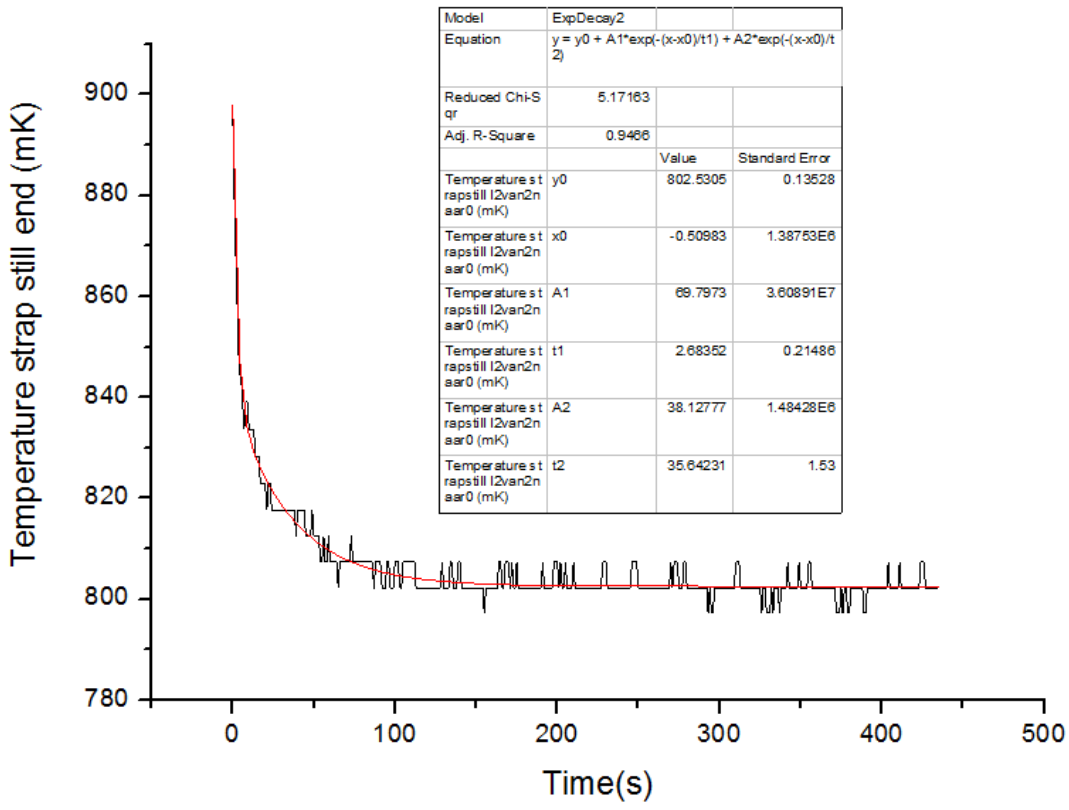

Appendix Fig.3: Top: normalized cool down from 4.9 mW to 3.6 mW. Bottom: cool down 0.9K to 0.8K.

10.4. Log-file of heat treatment by NORMA

Chargeprotocol voor NORMA IMS 20.03.2018 15:24:08 - 1 -

Chargegegevens

- Charge-ID	: 2018030036
- Beschrijving	: 2018-00133
- Order	:
- Charge in systeem	: 20.03.2018 11:21:10
- Charge uit systeem	: 20.03.2018 15:24:00
- Programma-aanduiding	: R.V.S. 316..
- Bijkomende programmainfo	: gloeien 1100 C.
- Klanten Nr.	:
- Datum	: 20.03.2018 11:20:00
- Order Nr.	: F020.748

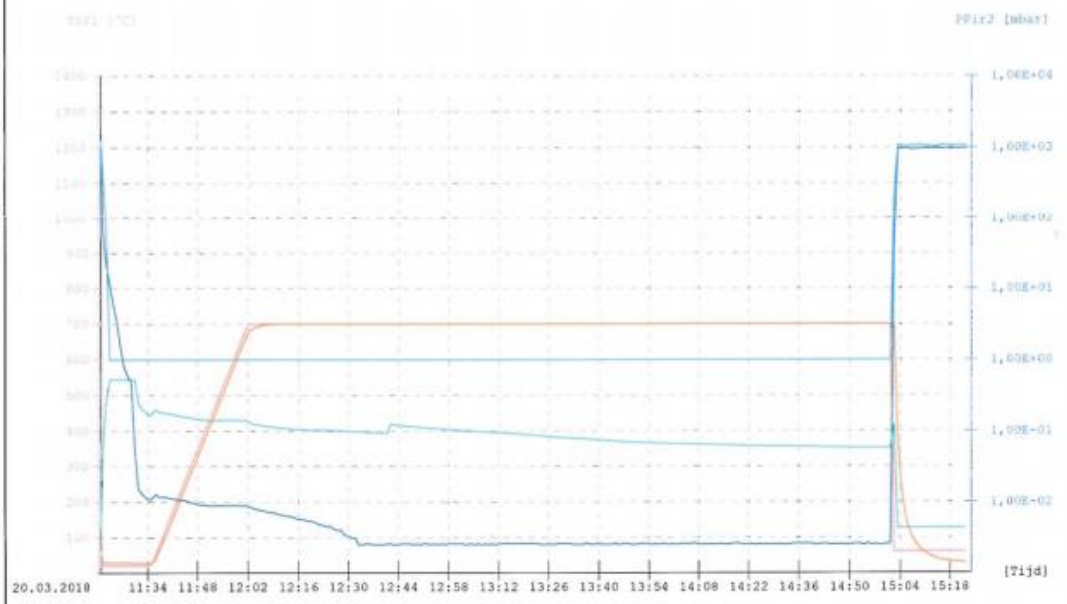

10.5. ECu-57 copper strap

NAGLER NORMALIEN

Copper (ECU)

EDM Copper 99,9%

DIN	ECU57 / 2.2065
Europe/EN	CU-ETP / CW004A

Gewichtsanteile:
Cu: 99,9 %
Sauerstoff: 0,005 bis 0,040 %

Produced by electrolytic refining, oxygen-containing (tough pitch) copper, with a very high conductivity for heat and electricity (in the soft state min. 57 m Ω-1 / mm). Very suitable for EDM electrodes, as well as in electrical engineering, electronics. Not suitable for brazing and welding Cu = 99.9% min. The electrical resistance is smaller than 0.01754 x Ω mm². Very good cold and hot-formable material. Excellent for mechanical and electrochemical polishing.

Use areas of ECU57:

Electrodes for spark erosion removal method. (EDM)
Components for the electronics
Heat dissipation in tools

General properties of copper:

Salmon-red color
Melting point: 1,083 ° C
Density / spec. Weight: 8,9 kg / dm
UV and corrosion resistance
High conductivity of electricity and heat
Excellent forming and workability
Standardized processing technique
No change under pressure, heat or cold
Hygienic (drinking water regulation DIN 50930)
Extreme stability against pressure and temperature fluctuations
Favourable price / performance and long life

Machanical properties approx (Cross-section dependent)

Tensile strength	*N/mm²*	200
Yield strength $R_{p0.2}$	*MPa*	160
Density	*m³*	8944
Melting point	*°C*	1083
Brinell hardness	*HB*	40
Tensile strength Strain hardened	*N/mm²*	400
Thermal conductivity	*W/km*	383
Electrical conductivity	*m Ω⁻¹*	57-59

10.6. Q&A Thermal model Henk van Weers

As the thermal dynamics of the LC-cooler turned out to be more complicated than first anticipated, the initial desire of thermal control of the existing setup became though to realize. Moreover, as we wanted to connect the thermal model to the existing thermal model of the DM-FPA (X-IFU), which was done in Open Modelica, the same software should be used for our thermal model. As time was short and the use of Open Modelica gave rise to more questions, the thermal model of the LC-cooler is still yet to be made. Henk van Weers, who is responsible for the creation of the thermal model of the DM-FPA, was willing to answer my burning questions towards thermal modelling in Open Modelica. A Q&A with Henk van Weers can be found here:

Q&A Thermal model:

Before I start answering the individual questions, I would like to give you (and others) a bit more background on why I am trying to setup the thermal model for the XIFU FPA in Modelica:

Finding a suitable implementation for an FPA lumped thermal model (over the complete development until flight) has been a bit of a search. Within Space instrumentation development several high-end thermal packages are used, such as ESATAN (originally developed by ESA, but now privately owned by ITP Engines UK), Thermica (part of the Systema suite developed by Airbus Space and defence in France) and Sinda (developed by MSC Software, US). CNES, our prime is using Thermica, our NASA colleagues use Sinda and ESA is using ESATAN. Problem with all of these packages is that they are quite costly. A single user ESATAN license for one year costs for instance about 10 KEuro. Furthermore it provides all kinds of options which we will not use for our FPA-DM (such as detailed radiative calculations). Another drawback is that it requires quite some knowledge of the software to make reliable models (as is the case with all modelling software packages). One major item I expect that we need to tackle within the XIFU FPA is the coupling between a mechanical dynamical model (lumped mass-spring model) coupled to a lumped element thermal model. This to see the impact of micro-vibrations on the temperature stability and thus detector performance. None of the high-end packages have a standard facility to handle such coupled models, as far as I know. This, plus the fact that any thermal lumped element model can be converted into an ESATAN, Thermica or Sinda format has lead me to choose the Modelica language for modelling the thermal (and later on thermal-dynamical) lumped element model of the FPA.

-Can you send me the Open Modelica code of the DM-FPA model?

Yes I can, it is actually not one model but rather a collection of models see contents of directory "FPA_Models". To be able to re-use various lumped thermal components in these models I collected them in a small library "ThermalCryogenics library 0.1", the version I used in SRON-XIFU-TN-2017-038 issue 2. I have attached this library and you locally save it (I placed it under c:\OpenModelica1.12.0-64bit\lib\omlibrary\). Then you can indicate OMEdit to standard load this library, under tab Tools->Options :

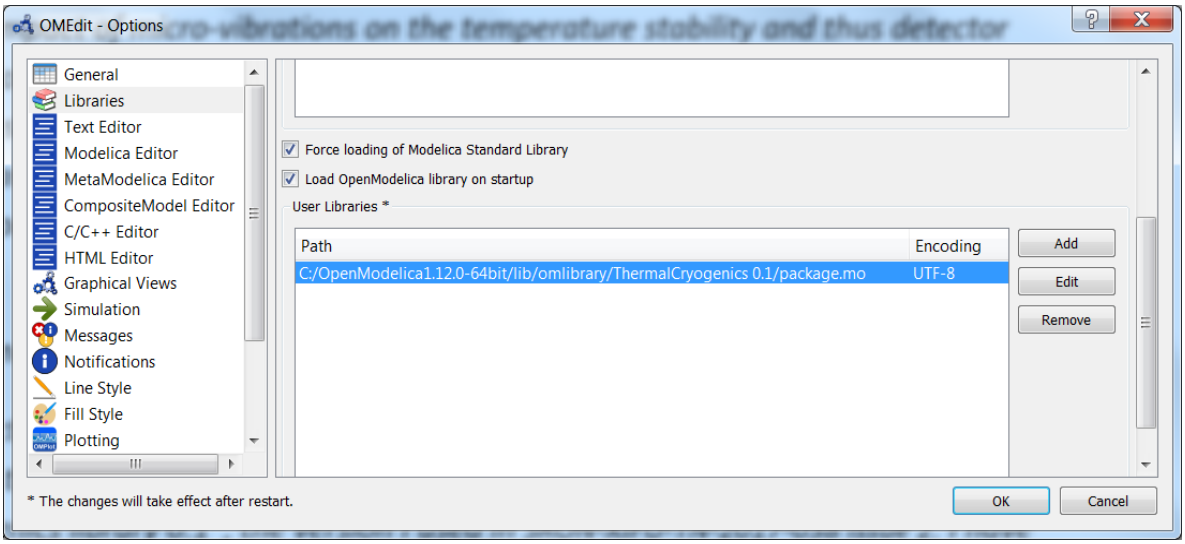

As you can see the within this library the material type is enclosed within the component models (an aluminum resistor is different from a niobium resistor). This is leading to issues when further discretizing the lumped heat-capacities into sub- elements: Each time the material of a part is changed the whole resistor/capacitor structure needs to change, while actually only the material is changed. After realizing this I am now re-writing the library is such a way that the capacitors and resistors are independent components (with a volume and A/l ratio respectively) and that a separate material model is assigned to these capacitors and resistors. For a discretized part you can then set one material for all capacitors and resistors in the part. Although I have started with this work it is still in progress. My current expectation is that I will only be able to complete this around end of April/begin May.

-You mention in section 1.4 I. that thermal properties are all highly temperature dependent. Moreover, you mention that Modelica is primarily intended for time domain analysis and is well suited implementation of these temperature dependencies and resulting non-linear equations.

The underlying codes/assumptions for the model you've made in Figure 2-1 are these indeed temperature dependent, i.e. are the thermistor and capacitors used in Figure 2-1 temperature dependent or approximated for a single temperature?

Within the Modelica models all heat capacities and conductances are indeed temperature dependent (Large signal model). See for instance " CryoHeatCapacities.mo" In this small thermal model you can see the implemented discontinuity at Tc for superconding heat capacities.

-In what way are the thermistors and capacitors linked to each other? I have multiple sources about thermal circuits where one source would model it as an RC network in "series" and the other source puts the RC network "parallel" to each other.

In principle when discritizing a single heat capacity to allow temperature gradients you can make a subdivision of the single capacity into multiple smaller capacities linked via resistances. The method used within ESATAN is the so called "far field method" See some papers I attached. In other methods one FEM element is modelled by multiple heatcapacities and resistors. In this case sometimes parallel networks are added which reduce the total amount of heat capacity of the element when a thermal gradient is applied over its nodes. I intend to use the far field method for further discretization, in order to be in line with ESATAN and Thermica.

-The heaters in the model have a fixed heat flow. Does the model/modelica allow for a dynamic heating process (as function of time) and if so, is this easily implementable in modelica?

Yes Modelica does allow these type of definitions. It allows continues time domain modelling and discrete time domain modelling (see for instance http://book.xogeny.com/behavior/discrete/measuring/). The solver is capable to detect events and adjust time stepping accordingly. See for instance (http://book.xogeny.com/behavior/discrete/bouncing/)

I used such a feature in the "ThreeLumpedCapacitance_pulse.mo" model where a heat pulse is applied to one of the heaters.

-In section 3.5 you give a realization of the (linearized) state space representation. Is this a result from the OpenModelica code or did you derive the representation yourself, i.e. by injecting a pulse/step function into the DM-FPA to obtain the transfer function from which a realization has been made?

Yes this is indeed a result from OpenModelica. I use the graphical editor OMEdit to build the model and see the graphical representations. For solving the models I use OMPython, which is a small python module that allows running the OMC compiler and solver to be run from within Python. This gives the flexibility to run a range of parameters for instance to do a sensitivity analysis. The state-space matrix results are provided back to Python. Within the Python environment you can then use the Python Control standard library to analyse all kind of properties of the linearized system.

-Page 19/Table 3-2. From the calculated DC gains how did you obtain the temperature stability requirements?

These requirements were not derived using this model, but rather an earlier hand calculation by Brian/Piet de Korte. The FPA thermal model demonstrates that with the foreseen design implementation we are compliant with this requirement.